AD_____

Award Number: W81XWH-06-1-0397

TITLE: Metabolic Mapping of Breast Cancer with Multiphoton Spectral and Lifetime Imaging

PRINCIPAL INVESTIGATOR: Long Yan

CONTRACTING ORGANIZATION: University of Wisconsin-Madison
Madison, WI 53706

REPORT DATE: March 2007

TYPE OF REPORT: Annual Summary

PREPARED FOR: U.S. Army Medical Research and Materiel Command
Fort Detrick, Maryland 21702-5012

REPORT DOCUMENTATION PAGE

Form Approved
OMB No. 0704-0188

1. REPORT DATE	2. REPORT TYPE	3. DATES COVERED
01-03-2007	Annual Summary	1 Mar 2006 – 28 Feb 2007

4. TITLE AND SUBTITLE

Metabolic Mapping of Breast Cancer with Multiphoton Spectral and Lifetime Imaging

5a. CONTRACT NUMBER

5b. GRANT NUMBER
W81XWH-06-1-0397

5c. PROGRAM ELEMENT NUMBER

6. AUTHOR(S)

Long Yan

Email: longyan@wisc.edu

5d. PROJECT NUMBER

5e. TASK NUMBER

5f. WORK UNIT NUMBER

7. PERFORMING ORGANIZATION NAME(S) AND ADDRESS(ES)

University of Wisconsin-Madison
Madison, WI 53706

8. PERFORMING ORGANIZATION REPORT NUMBER

9. SPONSORING / MONITORING AGENCY NAME(S) AND ADDRESS(ES)
U.S. Army Medical Research and Materiel Command
Fort Detrick, Maryland 21702-5012

10. SPONSOR/MONITOR'S ACRONYM(S)

11. SPONSOR/MONITOR'S REPORT NUMBER(S)

12. DISTRIBUTION / AVAILABILITY STATEMENT
Approved for Public Release; Distribution Unlimited

13. SUPPLEMENTARY NOTES
Original contains colored plates: ALL DTIC reproductions will be in black and white.

14. ABSTRACT

Currently we designed and implemented a combined spectral and lifetime imaging system which combines the benefits of multiphoton microscopy, spectral discrimination, lifetime analysis and temporal information. This system has efficiencies of > 50% and capability to collect broad spectrums (from 380nm-700nm). We determined the fluorescence source under our imaging condition is from NADH by this combined spectral and lifetime imaging system. Furthermore, we validated the accuracy of our lifetime analysis method. Our preliminary results of metabolic mapping in different human breast cell lines via fluorescence lifetime measurement of Co-Enzyme NADH showed very interesting results in differences of the lifetime and contribution of bound NADH between human normal breast cell line (MCF10a) and human breast cancer cell lines (T47D and MBA_MD_231). A 2-Deoxy-D-glucose (2DG) perturbation study is underway to link these finds with glycolysis.

15. SUBJECT TERMS
Breast Cancer, Metabolism, Lifetime, Spectra, Multiphoton

16. SECURITY CLASSIFICATION OF:			17. LIMITATION OF ABSTRACT	18. NUMBER OF PAGES	19a. NAME OF RESPONSIBLE PERSON
a. REPORT	b. ABSTRACT	c. THIS PAGE			19b. TELEPHONE NUMBER *(include area code)*
U	U	U	UU	58	USAMRMC

Standard Form 298 (Rev. 8-98)
Prescribed by ANSI Std. Z39.18

Table of Contents Page

INTRODUCTION:

Currently, little is known about the spectral and fluorescence lifetime signatures of key intrinsic fluorophores such as NADH and FAD within breast epithelial cells. We have reported a novel non-invasive method for deriving functional maps of oxidative cellular metabolism *in vivo* via measurement of the fluorescence lifetimes and the ratio of free to protein-bound NADH using two-photon fluorescence lifetime imaging microscopy (FLIM)(*1*). By dynamically imaging a normal MCF10a human breast cell line with sub-cellular resolution at an early, logarithmic and confluent phase of the cellular growth curve, we made the interesting observation that there is a progressive decrease in the fluorescence lifetime of both the free and protein-bound components of NADH and an increase in the short lifetime to long lifetime ratio of NADH with increasing confluence. Our studies suggest that fluorescence lifetime measurement of the bound and free states of NADH can allow for metabolic mapping of tumors and may provide a novel way to detect and characterize breast cancer invasion and progression.

The goal of this research is to apply a recently developed novel non-linear imaging modality(*2*), which combines current state of the art imaging techniques (fluorescence spectroscopy and fluorescence lifetime) with multiphoton microscopy into an integrated system. This system is designed to collect all the information in the fluorescence signal and exploit this information to demonstrate the potential for imaging endogenous fluorescence signatures in breast cancer cell models. We expect that this new combined spectral lifetime imaging modality will help for

characterization of breast cancer cells from cell culture based models to a relevant in vitro tumor-host environment and eventually to in vivo tumor models.

BODY:

In order to most effectively discriminate and characterize fluorescence sources in living samples, one needs to collect as much as information as possible such as intensity, spectral and lifetime information. Spectra can be used to discriminate between fluorophores on the basis of wavelength, and lifetime can be used to report on the microenvironment of fluorophores. The first task we have done is to design and implement a novel technique—combined spectral and lifetime imaging—which combines the benefits of multiphoton microscopy, spectral discrimination, lifetime analysis and allows for the simultaneous collection of all three dimensions of data along with spatial and temporal information. Our current spectrometer used a blazed, aberration corrected holographic diffraction grating which has efficiencies of > 50% and directly mounted on the side port of a Nikon microscope. This system has the capability to collect broad spectrums (from 380nm- 700nm) and instrument response for lifetime measurement is only 240ps. We have recently published our system in Biotechniques(*3*). The system is calibrated and helped us to confirm the fluorescence source from living cells under our imaging conditions (789nm 2-photon excitation) is indeed NADH. Many other research projects at the UW-Madison have benefited from this system because of its advantages for intrinsic and extrinsic fluorescence imaging. A paper reviewing these efforts has been accepted and is in press in the journal Microscopy and Microanalysis.

We were able to determine the fluorescence source under our imaging conditions is from NADH (bound and free forms) by comparing emission spectrum of NADH solution and MCF10a cells under same condition. Furthermore, we compared lifetime of NADH solution with literature and validated the accuracy of our lifetime analysis method.

Metabolic mapping in different human breast cell lines via fluorescence lifetime measurement of co-enzyme NADH was carried out. Upon the preliminary results, there are very interesting results in differences of the lifetime and contribution of bound NADH between human normal breast cell line (MCF10a) and human breast cancer cell lines (T47D and MBA_MD_231). Our preliminary results were presented in conference BIOS 2007 by The International Society for Optical Engineering.

2-Deoxy-D-glucose (2DG) is a molecule which has the 2-hydroxyl group replaced by hydrogen, so that it cannot undergo further glycolysis. Since NADH is involved into many metabolism pathways such as glycolysis, 2DG perturbation study is carried out. The results of this 2DG perturbation study may show a clue and help us to understand why there is the difference in the lifetime and contribution of bound NADH between human malignant cell lines and non-malignant cell line.

KEY RESEARCH ACCOMPLISHMENTS:

- Designed and implemented a novel fluorescence spectral and lifetime system and integrated into a multiphoton fluorescence excitation microscopy system

- Calibrated and characterized this fluorescence spectral and lifetime system and demonstrated the feasibility of fluorescence spectral and lifetime system
- Validated fluorescence source in cellular density study are from NADH by this fluorescence spectral and lifetime system under our imaging conditions.
- Carried out fluorescence lifetime measurement of 3 different cell lines under 3 different cells densities
- Carried out fluorescence lifetime data analysis, extracted NADH fluorescence lifetime results and characterized NADH fluorescence lifetime results with different cell types

REPORTABLE OUTCOMES:

Publications:

Long Yan, Curtis T. Rueden, John G. White, and Kevin W. Eliceiri, "Applications of combined spectral lifetime microscopy for biology", Biotechniques, 2006 September. 41(3), 249-257

Paolo P. Provenzano, Kevin W. Eliceiri, Long Yan , Aude Ada-Nguema, Matthew W. Conklin, David R. Inman, Patricia J. Keely, "Nonlinear optical imaging of cellular processes in breast cancer", Microscopy and Microanalysis. In Press.

Conference presentations:

Long Yan, Kevin. W. Eliceiri, Patricia J. Keely and John. G. White, "Combined spectral lifetime microscopy for in-vivo cell biology and cancer studies", The International Society for Optical Engineering, BIOS 2007, San Jose, California, USA, January, 2007

Long Yan Kevin. W. Eliceiri, Patricia J. Keely, Nirmala Ramanujam and John. G. White "Metabolic mapping of human breast cell lines via multiphoton fluorescence lifetime imaging of the coenzyme NADH", The International Society for Optical Engineering, BIOS 2006, San Jose, California, USA, January, 2006

CONCLUSION:

Fluorescence spectral and lifetime characterization of NADH may be used to reveal metabolic changes in vivo and has potential to be used as an early diagnostic tool for breast cancer. Preliminary studies in human breast non-malignant cell line and human breast malignant cell lines demonstrated that the differences in the fluorescence lifetime and contribution of NADH can be used to characterize tumor cell lines and thus has the potential to identify tumor cell lines from normal cell lines. This combined spectral and lifetime system has proved to be very useful in living cell imaging. However, the collection of simultaneous spectral and lifetime dimensions presents practical challenges of how to view and analyze these data, due to their large size and complex multidimensional structure. Thus future work will need to be done to find ways to optimize the collection and analysis of this complex data.

REFERENCES:

1. D. K. Bird *et al.*, *Cancer Res* **65**, 8766 (October 1, 2005, 2005).

2. D. K. Bird, K. W. Eliceiri, C. H. Fan, J. G. White, *Appl Opt* **43**, 5173 (Sep 20, 2004).

3. L. Yan, C. T. Rueden, J. G. White, K. W. Eliceiri, *Biotechniques* **41**, 249 (Sep, 2006).

APPENDICES: (Attach all appendices that contain information that supplements, clarifies or supports the text. Examples include original copies of journal articles, reprints of manuscripts and abstracts, a curriculum vitae, patent applications, study questionnaires, and surveys, etc.)

Nonlinear Optical Imaging of Cellular Processes in Breast Cancer

Paolo P. Provenzano[1,2], Kevin W. Eliceiri[2]*, Long Yan[2], Aude Ada-Nguema[1], Matthew W. Conklin[1,2], David R. Inman[1], Patricia J. Keely[1,2]

[1] *Department of Pharmacology,* [2]*Laboratory for Optical and Computational Instrumentation, University of Wisconsin, Madison, WI*

Running Title: Nonlinear Imaging in Breast Cancer

Prepared for *Microscopy and Microanalysis*

Submission Date: 04-19-06

Keywords: Multiphoton Excitation Microscopy, Second Harmonic Generation (SHG), Fluorescence Lifetime Imaging Microscopy (FLIM), Signal Transduction, Stromal Collagen, Breast Cancer, Nonlinear imaging

*Corresponding Author:
Laboratory for Optical and Computational Instrumentation
1675 Observatory Drive
Madison, WI 53706 USA
Fax: 608-262-4570
e-mail: eliceiri@wisc.edu

ABSTRACT

Nonlinear optical imaging techniques such as multiphoton and second harmonic generation microscopy used in conjunction with novel signal analysis techniques such as spectroscopic and fluorescence excited state life-time detection have begun to be used widely for biological studies. This is largely due to their promise to non-invasively monitor the intracellular processes of a cell together with the cell's interaction with its microenvironment. Compared to other optical methods these modalities provide superior depth penetration and viability and have the additional advantage in that they are compatible technologies that can be applied simultaneously. Therefore, application of these nonlinear optical approaches to the study of breast cancer holds particular promise as these techniques can be used to image exogeneous fluorophores such as GFP as well as intrinsic signals such as second harmonic generation from collagen and endogenous fluorescence from NADH or FAD. In this manuscript the application of multiphoton excitation, second harmonic generation, and fluorescence lifetime imaging microscopy to relevant issues regarding the tumor-stromal interaction, cellular metabolism, and cell signaling in breast cancer is described. Furthermore, the ability to record and monitor the intrinsic fluorescence and second harmonic generation signals provides a unique tool for researchers to understand key events in cancer progression in its natural context.

Abbreviations: extracellular matrix (ECM); green fluorescent protein (GFP); multiphoton laser scanning microscopy (MPLSM); multiphoton excitation (MPE); fluorescence lifetime imaging microscopy (FLIM); second harmonic generation (SHG); nicotinamide adenine dinucleotide (NAD(P)H referred to here as NADH) ; flavin adenine dinucleotide (FAD);

INTRODUCTION

Nonlinear optical imaging techniques such as multiphoton excitation microscopy (MPE), second harmonic generation (SHG), used in conjunction with fluorescence lifetime imaging microscopy (FLIM) provide powerful tools to image cellular processes both *in vitro* and *in vivo* (Denk et al. 1990; Brown et al. 2001; Campagnola et al. 2002; Zoumi et al. 2002; Brown et al. 2003; Cox et al. 2003; Eliceiri et al. 2003; Zipfel et al. 2003; Wang et al. 2005). The purpose of this manuscript is to demonstrate how the application of these three imaging modalities, used in concert to obtain multidimensional data, can help elucidate fundamental issues in breast cancer.

Multiphoton Excitation

Multiphoton laser scanning microscopy (MPLSM) builds upon the advantages brought about by the widespread introduction of confocal laser-scanning microscopy (Brakenhoff et al. 1985; White et al. 1987), which allows thick biological sections to be imaged imaged through optical sectioning. Multiphoton microscopy, first introduced by Denk and colleagues (Denk et al. 1990), is an alternative optical sectioning technique where fluorescence excitation is restricted to the plane of focus, with an effective imaging depth that can greatly exceed conventional confocal microscopy (Denk et al. 1990; Centonze and White 1998), while better maintaining viability after prolonged exposure to excitation (Squirrell et al. 1999). This is largely due to the fact that multiphoton excitation occurs via multiple low-energy (typically 650-1050 nm excitation) photons acting in concert to produce an emitted photon at the same wavelength as the corresponding single photon excitation, but with less scattering and a nonlinear dependence for fluorescent intensity (Denk et al. 1990; Centonze and White 1998; Diaspro and Sheppard 2002; Helmchen and Denk 2002). Accordingly, for the case of two-photon excitation

(TPE), the fluorescence intensity $I_f(t)$ is proportional to the square of the intensity of the laser light $I(t)$ [after (Diaspro and Sheppard 2002)]:

$$I_f(t) \propto \delta_2 I(t)^2 \propto \delta_2 P(t)^2 \left[\pi \frac{(NA)^2}{hc\lambda} \right]^2, \quad (1)$$

where δ_2 is defined as a molecular cross section that represents the dependence for the probability of TPE on the square of photon density, $P(t)$ is the laser power, NA is the numerical aperture, h is Planck's constant, c is the speed of light, and λ is the wavelength. Therefore, due to this quadratic dependence, and the fact that excitation only takes place when multiple low-energy photons are absorbed by a fluorophore, the probability of TPE outside the focal plane is low, resulting in the optical sectioning effect (Denk et al. 1990; Centonze and White 1998; Diaspro and Sheppard 2002; Zipfel et al. 2003); making MPLSM ideal for generating high-resolution images of introduced and/or endogenous fluorophores from deep inside live biological tissues.

Second Harmonic Generation

In contrast to the fluorescent emission resulting from multiphoton excitation, second harmonic generation arises from the laser field suffering a nonlinear, second-order, polarization when passing through non-centrosymmetric ordered structures (Freund and Deutsch 1986; Campagnola et al. 2002; Stoller et al. 2002; Cox et al. 2003; Mohler et al. 2003; Williams et al. 2005; Plotnikov et al. 2006), such as fibrillar collagen. In general form, this nonlinear polarization can be described as (Stoller et al. 2002; Mohler et al. 2003; Williams et al. 2005):

$$\mathrm{P} = \chi^{(1)} * \mathrm{E} + \chi^{(2)} * \mathrm{E} * \mathrm{E} + \chi^{(3)} * \mathrm{E} * \mathrm{E} * \mathrm{E} + \ldots, \quad (2)$$

where the polarization (P) and electric field (E) are vectors, and the nonlinear susceptibilities, $\chi^{(i)}$, are tensors. It is the second term in equation 2 that represents SHG. Since SHG is a conserved polarizing process, the resulting coherent wave is exactly half the incident wavelength, with the intensity of the

SHG signal proportional to the square of both I and $\chi^{(2)}$ (Shen 1989; Stoller et al. 2002; Mohler et al. 2003). As such, the SHG signal is proportional to the square laser intensity as well as the molecular concentration (Mohler et al. 2003), organization and orientation (Shen 1989; Williams et al. 2005) of the sample; allowing the acquisition of information regarding concentration and structure in biological materials. Furthermore, since multiphoton excitation and second harmonic generation can be executed simultaneously, yet still be differentiated due to their distinct emission signals, it provides a powerful tool for imaging heterogeneous biological tissues.

Fluorescence Lifetime Imaging Microscopy

Time-domain fluorescence lifetime imaging microscopy is a method to display the spatial distribution of excited state lifetimes (Lakowicz et al. 1992; van Munster and Gadella 2005), where nonlinear lifetimes (with respect to time) are measured at each pixel and presented as contrast. This fluorescent decay (lifetime) is often well described with the following multi-exponential function (Lee et al. 2001; Becker et al. 2004; Bird et al. 2005):

$$I_f(t) = \sum_{i=0}^{n} a_i \exp^{(-t/\tau_i)} + c = a_1 \exp^{-t/\tau_1} + a_2 \exp^{-t/\tau_2} + a_3 \exp^{-t/\tau_3} + ... + c \quad (3)$$

where $I_f(t)$ is the fluorescent intensity at some time t following the excitation pulse, n is the number of exponential terms needed to describe the signal well (typically 1 to 3), a is the fractional contribution of each of the components, τ is the fluorescence lifetime, and c is background light noise.

In contrast to fluorescent emission intensity (see Eq. 1), the fluorescence lifetime is independent of fluorophore concentration (Lakowicz et al. 1992; Becker et al. 2004; van Munster and Gadella 2005), providing an additional dimension of information that allows fluorophores to be distinguished or identified. Hence, by combining the advantages of multiphoton imaging discussed above with FLIM to realize multiphoton-FLIM (French et al. 1997; Bird et al. 2005; Parsons et al. 2005), an extra dimension of data can be obtained that can help distinguish or describe processes such

as fluorophore and signal identification, molecular activation state, molecular microenvironmental conditions, cellular metabolic state, protein-protein interactions, and protein-DNA interactions (French et al. 1997; Verveer et al. 2000; Harpur et al. 2001; Tadrous et al. 2003; Bird et al. 2004; Peter and Ameer-Beg 2004; Bird et al. 2005; Cremazy et al. 2005; Parsons et al. 2005; Peter et al. 2005). Since these processes are highly relevant to breast cancer the additional information obtained with multiphoton-FLIM is extremely valuable and provides a powerful tool to studying, identifying, and understanding cellular processes both *in vitro* and *in vivo*.

Application of Nonlinear Imaging in Cancer

The capacity to image live tumor cells in their native, as well as engineered, microenvironment significantly enhances our ability to understand cellular behavior and better understand tumor formation, progression, and metastasis. To this end, multiphoton excitation, second harmonic generation, and fluorescence lifetime imaging microscopy have all been successfully utilized to better identify, understand, and characterize cancer (Brown et al. 2001; Jain et al. 2002; Wang et al. 2002; Brown et al. 2003; Palmer et al. 2003; Tadrous et al. 2003; Wang et al. 2004; Bird et al. 2005; Parsons et al. 2005; Sahai et al. 2005; Skala et al. 2005). In particular, three-dimensional imaging of live tissues with MPLSM has been utilized with great success to better understand two fundamental issues in cancer biology *in vivo*, namely: vascular behavior and metastasis (Brown et al. 2001; Jain et al. 2002; Wang et al. 2002; Wang et al. 2005). Employing intravital imaging methodologies, assisted by the introduction of xenograft cells with an engineered fluorophore such as GFP (Brown et al. 2001; Wang et al. 2002), or multiple fluorophores (Sahai et al. 2005), these researchers have gained insight into single and collective cell behavior *in vivo* (Brown et al. 2001; Wang et al. 2002; Wang et al. 2004) and correlated imaged cell migration and metastasis *in vivo* with gene expression patterns associated with tumor cell invasion and metastasis (Wang et al. 2002; Wang et al. 2004).

In addition to the ability to image exogenous fluorophores, such as GFP, specific biological molecules can be imaged due to their endogenous fluorescence or intrinsic polarization (such as the SHG signal from collagen), allowing examination of native cells and the cell-extracellular matrix (ECM) interaction *in vivo*. Specifically, intrinsic fluorescence from molecules such as NADH, FAD, and tryptophan (Patterson et al. 2000; Huang et al. 2002; Zipfel et al. 2003; Kirkpatrick et al. 2005), as well as SHG signals from collagen, muscle, and microtubules (Campagnola et al. 2002; Mohler et al. 2003; Zipfel et al. 2003; Williams et al. 2005; Plotnikov et al. 2006), allow direct *in vivo* imaging of endogenous cells and matrices, in addition to providing non-invasive fluorescent markers for studying metabolism and disease state. For instance, early work by Chance and co-workers (Galeotti et al. 1970) examined NADH in tumor cells, while others correlated changes in NADH intensity and lifetime with metastatic potential (Pradhan et al. 1995) or metabolic changes in response to chemopreventive drugs (Kirkpatrick et al. 2005). Additional work utilizing FLIM on human breast cells further characterized the changes in the lifetime of NADH in live cells in culture (Bird et al. 2005), while separate work employed MPLSM to characterize squamous cell carcinoma *in vivo* largely via tumor associated changes in NADH intensity (Skala et al. 2005); demonstrating the utility of endogenous fluorescence for viewing and studying cancerous cells *in vivo*.

Endogenous signals arising from polarization (i.e. SHG) or time domain studies of endogenous fluorescence (i.e. FLIM) also provide powerful tools for imaging and studying cancer *in vivo*, yet to date, have received less attention than multiphoton excitation for imaging live cells within intact 3D tumor microenvironments. One notable exception is the work by Jain and colleagues (Brown et al. 2003), which characterized decreases in collagen in tumors by examining SHG signals after pharmacologic intervention. Furthermore, recent work by our research group utilizing SHG in conjunction with MPE and FLIM have characterized changes in cellular autofluorescence and collagen density in mammary glands and tumors, as well as particular collagen structures associated with live tumor cell invasion (unpublished observations). Hence, MPE, SHG, and FLIM are all capable of

identifying and characterizing key features of carcinoma *in vivo* and provide robust tools separately, or in conjunction with one another, to elucidate important aspects of cancer biology.

MATERIALS and METHODS

Cell Culture

T47D cells were obtained from the American Type Culture Collection; MDA-MB-231 cells were a kind gift from Dr. Alan Rapraeger (University of Wisconsin); COS-7 cells were obtained as a generous gift from Dr. Richard Anderson (University of Wisconsin, Madison, WI). In certain experiments MDA-MB-231 or COS-7 were transfected with either EGFP, EGFP-Vinculin, EGFP-R-Ras, EGFP-Cdc42(WT), EGFP-Cdc42(61L), or EGFP-Cdc42(17N), and as indicated in the text. EGFP-Vinculin was a kind gift from Dr. Anna Huttenlocher, (Univ. of Wisconsin), EGFP-R-Ras was subcloned into the EGFP-C1 vector, and cdc42 constructs were a kind gift from Dr. A.R. Howitz (University of Virginia). T47D cells were cultured at 37°C with 10% CO_2 while being maintained RPMI supplemented with 10% fetal bovine serum and insulin (8 μg/mL). MDA-MB-231 cells were maintained in DMEM supplemented with 10% fetal bovine serum and cultured at 37°C with 10% CO_2. COS-7 cells were maintained in DMEM (containing high glucose, L-glutamine, sodium pyruvate and pyridoxine hydrochloride) plus 10% fetal bovine serum at 37°C with 5% CO2.

Cells were cultured and imaged under standard 2D conditions or within 3D collagen matrices. For 3D culture cells were cultured within a 2.0 mg/mL type-I collagen gel (rat-tail collagen solution, BD Biosciences) neutralized with 100 mM HEPES in 2X PBS. Following gel polymerization for 1 hour, gels were soaked in cell specific media (described above) and maintained at 37°C with 10% CO_2 until imaged as described in the text.

Mammary Tumors

All animal experiments were approved by the institutional animal use and care committee and meet N.I.H. guidelines for animal welfare. To generate mammary tumors polyoma middle T (PyVT) mice (Lin et al. 2003) were employed.

Instrumentation

For all microscopy experiments reported herein, two separate custom designed multiphoton systems were employed at the University of Wisconsin LOCI laboratory (Wokosin et al. 2003; Bird et al. 2004; Bird et al. 2005). The first system is a multiphoton laser scanning optical workstation (Wokosin et al. 2003) constructed around a Nikon Eclipse TE300 that facilitates multiphoton excitation, SHG, and FLIM. All SHG imaging was performed on this microscope and was detected from the back-scattered SHG signal (Williams et al. 2005). A 5W mode-locked Ti:sapphire laser (Spectra-Physics-Millennium/Tsunami) excitation (laser field) source producing around 100fs pulse widths was tuned to wavelengths between 780 or 900 nm. The beam was focused onto the sample with a Nikon 60X Plan Apo water-immersion lens (N.A. =1.2). Multiphoton and SHG signals were discriminated with 464 nm (cut-on) long pass and 445 nm narrow band pass filters, while GFP signals were isolated with a 480-550 nm (band-pass) filter (all filters: TFI Technologies, Greenfield, MA). Intensity and FLIM data were collected by a H7422 GaAsP photon counting PMT (Hamamatsu) connected to a time correlated single photon counting (TCSPC) system (SPC-730, Becker & Hickl).

The second microscope has been recently described in detail (Bird et al. 2004; Bird et al. 2005) and allows generation of multiphoton excitation intensity images in conjunction with FLIM images. In short, the system is built around an inverted microscope (Diaphot 200, Nikon, Melville, NY) possessing a Bio-Rad MRC-600 confocal scanning unit (Bio-Rad, Hercules, CA) with source illumination from a Ti:Sapphire mode-locking laser (Coherent Mira, Coherent, Santa Clara, CA)

pumped by an 8-W solid-state laser (Coherent Verdi) to generate pulse widths of approximately 120 fs at a repetition rate of 76 MHz, with a tuning range of ~700–1000 nm. The confocal scanning unit produces a focused scanning spot that moves across the focal plane of the imaging objective after which the laser beam is transmitted to the microscope through a transfer lens (01LAO159, Melles Griot, Rochester, NY) and impinges on a dichromatic mirror (650DCSP, Chroma, Inc., Rockingham, VT) that directs incident illumination to the imaging objective (60X oil immersion, 1.4 NA, Nikon) while allowing the emitted visible fluorescent light to be transmitted to a fast photon-counting detector (PMH-100, Becker & Hickl). FLIM images were acquired with an electronic system for recording fast light signals by time correlated single photon counting (SPC-830, Becker & Hickl).

Acquisition for both MPLSM systems was done with WiscScan (Nazir et al. 2006) a lab developed software acquisition package that can control both the MPLSM and FLIM collection. Image analysis for combined (and separated) MPE-SHG was performed with ImageJ (Abramoff et al. 2004) and VisBio (Rueden et al. 2004) software. Fluorescent lifetime analysis was carried out with SPCImage (Becker & Hickl), which can fit fluorescent decay data with the exponential function (Eq. 3), for one, two, or three terms, and sum individual photon counts for each pixel to construct a contrast image. The incomplete model approach in SPC Image (ref SPC Image manual) was used to compensate for instances where the fluorescence decay is slow compared to the time window defined by the repetition rate of the laser system.

RESULTS and DISCUSSION

Relevant issues in Breast Cancer

It is estimated that 1 in 7 women have a lifetime probability of developing breast cancer and that in the year 2005 approximately 270,000 women will be diagnosed with breast cancer with an overall mortality rate of ~15% and lower survival associated with invasive and metastatic cancer

(American Cancer Society annual statistics; www.cancer.org). As such, techniques and tools to detect, characterize, study, and combat breast cancer are of great significance.

One of the largest risk factors for developing breast carcinoma is high breast tissue density (Boyd et al. 2002). Dense breast tissue is linked to a four-to-six fold increased risk of breast carcinoma (Boyd et al. 1998; Boyd et al. 2001), and it is known that high breast density is associated with increased collagen deposition and content (Guo et al. 2001). Therefore understanding epithelial-stromal (-collagen) interactions is of great relevance, and this importance is further highlighted by information that improper stromal-epithelial interactions can promote tumorigenesis (Ronnov-Jessen et al. 1995; Elenbaas et al. 2001; Tlsty and Hein 2001) and that metastatic breast carcinoma cells migrate away from tumors along collagen fibers (Wang et al. 2002). Moreover, aberrant signal transduction, altered metabolic state, genetic mutations, and altered transcriptional profiles have all been associated with carcinoma formation, progression, and metastasis (Hagios et al. 1998; Hanahan and Weinberg 2000; Jacks and Weinberg 2002; Muti 2004; Rangarajan et al. 2004; Condeelis et al. 2005; West et al. 2005). Therefore, as indicated in the previous section, MPE, SHG, and FLIM (or FRET-FLIM) either individually or in combination are very well suited to address important issues associated with each of these important areas of breast cancer research by utilizing both introduced (i.e. fluorescent probes, FRET probes in FRET-FLIM etc.) or endogenous (i.e. NADH, collagen etc.) signals. Examples of this utility are illustrated below.

Breast Cancer Related Tumor-Stromal Interactions

Understanding tumor-stromal interactions, both *in vitro* and *in vivo*, is an important aspect of the study of tumor formation and progression since stromal-epithelial interactions play a critical role in both tumorigenesis and metastasis (Ronnov-Jessen et al. 1995; Elenbaas et al. 2001; Tlsty and Hein 2001; Wang et al. 2002; Sato et al. 2004; West et al. 2005), and patients with collagen-dense breast tissue possess an increased risk of breast carcinoma (Boyd et al. 1998; Boyd et al. 2001). To help

elucidate the mechanisms associated with tumor-stromal interactions in breast cancer, optical imaging modalities that allow deep imaging of live tissue are of great utility. As seen in Figure 1, combined MPE and SHG facilitate viewing of intact live mammary tumor tissue. Figure 1 represents six planes of a 30-plane z-stack (10 μm steps; 300 μm total range), obtained at 890 nm excitation, which clearly shows collagen surrounding and within the tumor (i.e. SHG signal), as well as endogenous tumor cell fluorescence (i.e. MPE). Importantly, variations in both collagen structure and tumor cell autofluorescence across and within imaging planes can be simultameously acquired. Additionally, changes in local and global collagen density and specific stromal structures that influence tumor cell behavior can be obtained and defined (unpublished results). Hence, by studying the combined MPE/SHG signals in unfixed, unstained, non-sectioned tissues, the structure and composition of the stroma, as well as the degree and type of endogenous tumor-stromal interaction can be obtained.

To further differentiate signals (i.e. biological components) of the tumor, specific filtering techniques can be employed. By exploiting the fact that MPE excitation obeys the fundamental physical relationship of energy loss after excitation (i.e. emission of a lower energy, longer wavelength, photon following excitation by a higher energy photon) while SHG signals are exactly half of the excitation wavelength, the MPE and SHG signals can be separated (Figure 2). Following excitation of live mammary tumor tissue at 890 nm (a wavelength that produces endogenous cellular fluorescence and SHG of type I collagen) a 464 nm (cut-on) long pass filter was used to isolate the MPE signal while a 445 nm narrow band pass filter was used to separate the signal resulting from SHG. This approach allows clear visualization of the structure and organization of collagen in the stroma as well as the presence and arrangement of stromal fibroblast-looking cells surrounding less fluorescent epithelial tumor cells (Figure 2). Stromal cells clearly possess a more mesenchymal phenotype, demonstrate a greater fluorescent intensity, and associate with the collagenous stroma, with cells often aligned with collagen fibers. Thus, the use of combined MPE/SHG has the potential to help

identify and differentiate additional features that are either not obtainable or not easily obtained with more traditional fluorescent microscopy techniques. Furthermore, the fact that collagen signals primarily arise from the conserved SHG polarization following high wavelength (i.e. 860-920 nm) excitation, FLIM can be used to image and identify collagen (and other SHG generating proteins), as wells as fluorescent signals from live cells (Figure 3). Since SHG is a conserved polarization processes, the resulting signal following excitation has a theoretical lifetime of zero (i.e. no lifetime), while fluorescent signals have a lifetime that are fluorophore and microenvironment dependent. For example, mathematical analysis using a one or two-term exponential model (Eq. 3) of 10 locations that appear to be collagen structures in Figure 3 indicate that 99.3 ± 2.3% (a_1) of the lifetime signal (τ_1) is similar to the calibrated instrumental response function, indicating an essentially zero lifetime, signifying the signal results from SHG. In contrast, examination of fluorescent lifetime characteristics of tumor cells in Figure 3 indicates two distinct lifetime components, $\tau_1 = 0.243 \pm 0.032$ and $\tau_2 = 2.61 \pm 0.292$ (n=6 locations; mean ± s.d.) with a fractional ratio a_1:a_2 of 3.99 (Figure 3c), that represent different fluorescent molecules or different micro-environmental conditions and/or protein association states for the fluorophore (see Results and Discussion sections on *Metabolism* and *Signaling*). Hence FLIM allows identification of different proteins by supporting the concept that the majority of collagen signals arise from SHG at the correct excitation, which differs from the endogenous fluorescent signals occurring in live cells. Moreover, we are able to obtain MPE and SHG simultaneously and FLIM sequentially on the same system, providing powerful multidimensional data to analyze the tumor-stromal interaction in live tissue.

In addition to the powerful data obtained from live tissue imaging with MPE, SHG, and FLIM, significant understanding can be gained by applying these technologies to more controllable *in vitro* systems. For instance, studying breast epithelial cells within reconstituted three-dimensional (3D) matrices *in vitro* (Keely et al. 1995; Wozniak et al. 2003) provides a potent and relevant model system

for understanding cell behavior *in vivo*, particularly the epithelial-stromal interaction. For instance, studies on breast epithelial cells in 3D have demonstrated that improper regulation of integrin behavior, integrin mediated adhesion to the ECM, and adhesion mediated signaling profoundly influence cell signaling that can result in a more transformed phenotype (Keely et al. 1995; Wozniak et al. 2003; Paszek et al. 2005). Furthermore the physical act of tumor cell invasion and metastasis islargely, but not solely, regulated by integrins and focal adhesion signaling (Friedl and Wolf 2003; Friedl et al. 2004), with staining for β_1 integrin (a primary collagen receptor) localized at the leading edge of migrated melanoma cells from 3D tumor explants (Hegerfeldt et al. 2002; Friedl et al. 2004). A similar behavior can be seen in live breast carcinoma cells. Inspection of live highly migratory MDA-MB-231 invasive breast carcinoma cells within reconstituted 3D collagen matrices further highlights the cell-matrix interaction via 3D-matrix adhesions (Figure 4). Simultaneous imaging of GFP-Vinculin with MPE and the collagen gel with SHG reveals vinculin positive 3D-matrix adhesion at the cell-ECM interface. Early morphology of MDA-MB-231(GFP-Vinculin) cells seeded into collagen matrices after three hours (Figure 4a-c) indicates that the cells have not fully spread and exhibit vinculin positive filopodia-like structures that interact with collagen fibrils (see Figure 4c). This early interaction is likely an early step in cell anchorage and spreading, followed by contractility-mediated reorganization of the ECM, and ultimately migration. As such, examination of migratory MDA-MB-231(GFP-vinculin) cells after 24 hours in the 3D matrices show aligned collagen fibers associated with vinculin localization (Figure 4d-f), which are similar to results from melanoma cells in 3D collagen gels *in vitro* (Hegerfeldt et al. 2002; Friedl et al. 2004). Hence, simultaneous imaging of cellular processes and matrix organization and structure with combined MPE/SHG not only facilitates imaging of non-native and endogenous signals *in vivo*, but also provides a robust tool to study tumor-stromal interactions in live (unfixed, unstained, non-sectioned) cells *in vitro*, which can further our understanding of the *in vivo* condition.

Breast Cell Metabolism

Intrinsic fluorescence allows imaging of cells and tissues in their native environment, often conferring an advantage over imaging an introduced fluorophore when viewing biological structures in a relatively unperturbed environment is desired. Moreover, changes in metabolic status can be indicative of a diseased state (Galeotti et al. 1970; Pradhan et al. 1995; Pitts et al. 2001; Katz et al. 2002; Palmer et al. 2003; Kirkpatrick et al. 2005). For example, differences in NADH have been used to differentiate normal and cancerous epithelial tissues (Skala et al. 2005) with NADH intensity and lifetime altered with metastatic potential (Pradhan et al. 1995); and specific metabolic changes in NADH and tryptophan in response to chemopreventive drugs has been reported (Kirkpatrick et al. 2005).

Since biological tissues are heterogeneous, excitation often results in emission from multiple fluorophores with overlapping spectra. Therefore understanding the spectral properties of key fluorophores that correlate with specific cellular activity and that utilize specific excitation wavelengths as a tool to image endogenous structures are of great utility. While multiple sources of biological autofluorescence exist (see (Ramanujam 2000; Zipfel et al. 2003)), three strong (primary) sources of cellular autofluorescence are NADH (maximum λ_{ex}/ λ_{em}: 350/450 nm), FAD (maximum λ_{ex}/ λ_{em}: 450/535 nm), and tryptophan (maximum λ_{ex}/ λ_{em}: 280/340 nm). Figure 5 illustrates changes in breast tumor cell and matrix fluorescent intensity and localization as a function of excitation wavelength. At λ_{ex} = 780 nm, a wavelength that is close to the ideal two-photon absorption peak of NADH, a reasonably homogeneous pattern of endogenous cellular fluorescence in the cytoplasm is clearly visible (Figure 5a). However, as the excitation wavelength is increased in 20 nm increments to 880nm, changes in fluorescent intensity and localization can be discerned and the emergence of collagen SHG signal at λ_{ex} = 860-880 can be detected (Figure 5); likely indicating changes in emission

transitioning from two-photon excitation of NADH to FAD and possibly a relatively small three-photon excitation of tryptophan and/or three-photon excitation of a lower 260nm peak for NADH.

In order to study changes in cellular metabolism in a more homogeneous and controllable system, MPE and FLIM can be applied to normal and cancerous breast cells *in vitro*. Previous work in the "normal" MCF10A human breast cell line demonstrated that FLIM is useful to study the reduction/oxidation state of intracellular NADH by determining the ratio of free (τ_1) and protein bound (τ_2) NADH. Importantly, the ratio of free and protein bound NADH correlates to metabolic state and growth conditions (Bird et al. 2005). Figure 6 represents a fluorescence lifetime image of T47D breast carcinoma cells acquired at λ_{ex} = 740 nm in a two-dimensional environment with the color map representing the weighted average of the short and long components of NADH: $\tau_m = (a_1\tau_1 + a_2\tau_2) / (a_1 + a_2)$. The key advantage of utilizing FLIM is that the lifetime is independent of fluorophore (NADH in this case) concentration and clearly demonstrates the ability to image pertinent metabolic conditions in relevant breast carcinoma cells. In addition, FLIM facilitates the imaging and analysis of breast carcinoma cells in model 3D environments (Figure 7) and live mammary tissue and tumors (see Figure 3). Figure 7 represents MDA-MB-231 breast carcinoma cells in 3D collagen gels imaged at λ_{ex} = 890 nm. Again the color map represents the weighted average of the two-term model components and validates the ability to detect changes in cellular lifetime in highly invasive breast carcinoma cells. Hence, imaging the cellular fluorescence lifetime combined with MPE/SHG to study cell metabolism in conjunction with tumor-stromal interactions not only provides images of endogenous structure both *in vitro* and *in vivo*, but can also provide a robust tool to study changes in metabolism associated with disease state, complex cell behavior associated with tumor formation and progression, and the response to chemotherapeutic compounds.

Imaging Signaling Events Relevant to Breast Cancer

Aberrant cell signaling events and the signaling pathways associated with changes in cell survival, proliferation, and the transformed phenotype are critical phenomena that need to be elucidated in breast cancer. Although many studies have utilized GFP tagged signaling approaches to better understanding cellular processes with standard fluorescence and confocal microscopy (for example see (Lippincott-Schwartz et al. 2001; Zhang et al. 2002; Lippincott-Schwartz and Patterson 2003)), less work has been performed utilizing MPE of fluorescently-tagged signaling molecules in live cells, particularly utilizing combined MPE and SHG in 3D. However, several works have shown that MPE can be used in live cells to better understand key signaling events and other cellular processes (Strome et al. 2001; Robu et al. 2003; Poteryaev et al. 2005; Squirrell et al. 2006). In Figure 8, MDA-MB-231 were transfected with either GFP, or GFP tagged wild-type (wt), constitutively active (61L), or dominant negative (17N) constructs of cdc42. Live cells within type I collagen gels were imaged with combined MPE/SHG at λ_{ex} = 890 nm to detect changes in cell morphology and tagged-cdc42 localization as well as cell-induced changes in collagen gel microstructure (Figure 8). After six hours within 3D collagen gels, cells expressing constitutively active cdc42(61L) were more spread and formed more cell protrusions than either either control GFP cells or cells expressing dominant negative cdc42(17N) form and have began to align the collagen matrix (Figure 5a-c). Moreover, cells with active cdc42(61L) had begun to organize and align the collagen matrix with clear cell matrix interactions while cdc42(17N) expressing cells had not (Figure 5a-c). Of additional note, cells expressing wild-type cdc42 (GFP-cdc42(WT)) possessed long cell protrusions compared to control GFP cells but were not as spread as cdc42(61L) cells (Figure 5d,e), possibly indicating that these cells overexpress cdc42 compared to control GFP cells, further suggesting that cellular protrusion (filopodia) and cell spreading correlates to the amount of active cdc42. Combined with the early

filopodia-matrix interactions at three hours (Figure 4) these data may suggest that activated cdc42 (which is known to regulate filopodia protrusion (DeMali and Burridge 2003; Jaffe and Hall 2005) results in increased early matrix interactions resulting in a more spread cell by six hours. However, additional studies are required to better understand the temporal relation of cell morphology and signaling in 3D environments. Yet, Figure 8 clearly demonstrates the ability of combined MPE/SHG to image relevant signaling events in live breast carcinoma cells and their interaction with, and modulation of, the extracellular matrix.

Hence, recent advances in imaging allow the elucidation of signaling events in live cells with increased spatial and temporal resolution. Temporal studies of molecules tagged with GFP or other chromophores tracked over time are of great significance to understanding fundamental processes in breast cancer. For instance, localization to the plasma membrane is of particular significance for several key signaling molecules that traffic between the cytosol and membrane, such as the Rho GTPases, or within membrane bound endosomal compartments, such as Rab GTPases. Moreover, it is widely believed that the plasma membrane contains subdomains that contain differing lipid compositions, such as lipid microdomains or lipid rafts. However, the successful imaging of these domains has been generally rather elusive, but may be possible through nonlinear optical techniques, such as multiphoton FLIM, which provides information regarding the local microenvironment. We have found that the use of FLIM to monitor the spatial localization of GFP-tagged molecules has resulted in a novel elucidation of sub-domains within sites of plasma membrane localization. For example, use of MPE at 900 nm to image GFP-tagged constitutively active R-Ras, a member of the Ras family of GTPases that is relevant to breast cell behavior (Keely et al. 1999; Wozniak et al. 2005; Ada-Nguema et al. 2006), demonstrates localization of R-Ras to sites of active membrane protrusion (Figure 9a) in easily manipulated COS-7 cells. However, the same image analyzed and then color mapped for the fluorescent lifetime of the GFP-R-Ras demonstrates distinct domains along the protruding membrane that are not observed with MPLSM alone (Figure 9b,c). Although we currently

do not know whether these subdomains represent lipid microdomains, biochemical data supports the partitioning of R-Ras into lipid microdomains (data not shown), suggesting that FLIM could be a useful tool to image and identify these regions in live cells.

Similar results are obtained when imaging fluorescent molecules that intercalate into membranes, such as filipin. Imaging of filipin via confocal microscopy (not shown) or via MPE demonstrates uniform staining of the entire plasma membrane, with no elucidation of additional structure or microdomains (Figure 10a). However, when the same image is analyzed by FLIM, the presence of two populations of filipin molecules emerges (Figure 10b). Again, these distinct regions likely represent two physically or biochemically distinct environments, and are consistent with the partitioning of filipin into cholesterol rich regions. Indicating that the use of FLIM has the potential to identify and image additional features within cells that are not apparent with intensity data alone. Consequently, additional studies combining MPE, SHG, and FLIM to better define the nature of key cell signaling events, cell-matrix regulated or regulating signals, and specific plasma membrane subdomains are ongoing.

Hence, using MPLSM to obtain MPE, SHG, and FLIM (or FRET-FLIM) either individually or in combination provides the potential to help elucidate fundamental processes in breast cancer. By utilizing fluorescent probes, endogenous fluorescence, biological protein polarizations, and FRET technologies, in conjunction with standard biochemical and molecular biology techniques, important questions in cancer research can be addressed in a more in depth and unperturbed manner. Thus, the combined utility of the multidimensional information obtained from these imaging modalities when applied to cells and tissues provides a relatively unique view of the relevant biological system that can explain mechanisms of tumor formation and progression.

Future Directions: Instrumentation, Bioinfomatics, and Analysis

MPLSM is emerging as a powerful tool to understand breast cancer in cells, animal models, and harvested human tumor tissue. Furthermore recent advances in detector technology hold great promise for improved detection of weakly fluorescent samples and combined detection of dimensions other than intensity such as spectral and lifetime (see (Bird et al. 2004) and Figure 11). These techniques, possibly combined with improved fluorescent probes (Zhang et al. 2002), are being developed for enhanced detection of autofluorescence and exogenous fluorophores as well as FRET and FRET-FLIM experimentation. In conjunction with these advances in microscopy technologies, development of publicly available image visualization and analysis tools such as the Open Microscopy Environment (Eliceiri and Rueden 2005; Goldberg et al. 2005), VisBio (Rueden et al. 2004) and ImageJ (Abramoff et al. 2004) are critical to provide image informatics infrastructure for the dissemination, analysis and visualization of multidimensional image data.

Furthermore, since MPLSM, and all of the associated imaging modalities (MPE, SHG, FLIM etc.) do not require a tissue biopsy to be fixed, sectioned, or stained there is potential for MPLSM not only to serve a valuable research tool, but also as a diagnostic tool. The ability to image freshly harvested tissue for pathological evaluation could be of great clinical utility and could provide multiple sets of information (*i.e.* metabolic state, tumor cell phenotype, stromal composition etc.) in a single imaged tumor volume. Moreover, the possibility of MPLSM as a clinical diagnostic tool must be considered. However for MPLSM to be a clinical diagnostic tool, the technique needs to improve in both its depth penetration and the mode through which it is delivered. Adaptive-Optics based multiphoton (Marsh et al. 2003) has potential to greatly increase the depth penetration of MPLSM by the use of optics that can change their wavefront in response to changes in refractive index in tissue. However there is not yet a practical implementation for MPLSM. Nonetheless, in the future, MPLSM does have the potential to be applied in vivo as a diagnostic tool through multiphoton fluorescence endoscopy (Bird and Gu 2002; Bird and Gu 2002; Bird and Gu 2003; Jung and Schnitzer 2003;

Flusberg et al. 2005). As such it is feasible that MPLSM has the potential to be a real-time diagnostic tool for early cancer detection and possibly treatment.

ACKNOWLEDGMENTS

The authors thank Dr. John White for his helpful comments and guidance regarding this work. This work was supported by grants from the DOD-CDMRP/BCRP: W81XWH-04-1-042 to P.P.P, the S.G. Komen Foundation: BCTR02-1841 and NIH: CA076537 to P.J.K. and NIH NIBIB: R01-EB000184 to K.W.E.

REFERENCES

Abramoff, M. D., Magelhaes, P. J. and Ram, S. J. (2004). "Image Processing with ImageJ." Biophotonics International **11**(7): 36-42.

Ada-Nguema, A. S., Xenias, H., Sheetz, M. P. and Keely, P. J. (2006). "The small GTPase R-Ras regulates organization of actin and drives membrane protrusions through the activity of PLC{epsilon}." J Cell Sci **119**(Pt 7): 1307-19.

Becker, W., Bergmann, A., Hink, M. A., Konig, K., Benndorf, K. and Biskup, C. (2004). "Fluorescence lifetime imaging by time-correlated single-photon counting." Microsc Res Tech **63**(1): 58-66.

Bird, D. and Gu, M. (2002). "Fibre-optic two-photon scanning fluorescence microscopy." J Microsc **208**(Pt 1): 35-48.

Bird, D. and Gu, M. (2002). "Resolution improvement in two-photon fluorescence microscopy with a single-mode fiber." Appl Opt **41**(10): 1852-7.

Bird, D. and Gu, M. (2003). "Two-photon fluorescence endoscopy with a micro-optic scanning head." Opt Lett **28**(17): 1552-4.

Bird, D. K., Eliceiri, K. W., Fan, C. H. and White, J. G. (2004). "Simultaneous two-photon spectral and lifetime fluorescence microscopy." Appl Opt **43**(27): 5173-82.

Bird, D. K., Yan, L., Vrotsos, K. M., Eliceiri, K. W., Vaughan, E. M., Keely, P. J., White, J. G. and Ramanujam, N. (2005). "Metabolic mapping of MCF10A human breast cells via multiphoton fluorescence lifetime imaging of the coenzyme NADH." Cancer Res **65**(19): 8766-73.

Boyd, N. F., Dite, G. S., Stone, J., Gunasekara, A., English, D. R., McCredie, M. R., Giles, G. G., Tritchler, D., Chiarelli, A., Yaffe, M. J. and Hopper, J. L. (2002). "Heritability of mammographic density, a risk factor for breast cancer." N Engl J Med **347**(12): 886-94.

Boyd, N. F., Lockwood, G. A., Byng, J. W., Tritchler, D. L. and Yaffe, M. J. (1998). "Mammographic densities and breast cancer risk." Cancer Epidemiol Biomarkers Prev **7**(12): 1133-44.

Boyd, N. F., Martin, L. J., Stone, J., Greenberg, C., Minkin, S. and Yaffe, M. J. (2001). "Mammographic densities as a marker of human breast cancer risk and their use in chemoprevention." Curr Oncol Rep **3**(4): 314-21.

Brakenhoff, G. J., van der Voort, H. T., van Spronsen, E. A., Linnemans, W. A. and Nanninga, N. (1985). "Three-dimensional chromatin distribution in neuroblastoma nuclei shown by confocal scanning laser microscopy." Nature **317**(6039): 748-9.

Brown, E., McKee, T., diTomaso, E., Pluen, A., Seed, B., Boucher, Y. and Jain, R. K. (2003). "Dynamic imaging of collagen and its modulation in tumors in vivo using second-harmonic generation." Nat Med **9**(6): 796-800.

Brown, E. B., Campbell, R. B., Tsuzuki, Y., Xu, L., Carmeliet, P., Fukumura, D. and Jain, R. K. (2001). "In vivo measurement of gene expression, angiogenesis and physiological function in tumors using multiphoton laser scanning microscopy." Nat Med **7**(7): 864-8.

Campagnola, P. J., Millard, A. C., Terasaki, M., Hoppe, P. E., Malone, C. J. and Mohler, W. A. (2002). "Three-dimensional high-resolution second-harmonic generation imaging of endogenous structural proteins in biological tissues." Biophys J **82**(1 Pt 1): 493-508.

Centonze, V. E. and White, J. G. (1998). "Multiphoton excitation provides optical sections from deeper within scattering specimens than confocal imaging." Biophys J **75**(4): 2015-24.

Condeelis, J., Singer, R. H. and Segall, J. E. (2005). "The great escape: when cancer cells hijack the genes for chemotaxis and motility." Annu Rev Cell Dev Biol **21**: 695-718.

Cox, G., Kable, E., Jones, A., Fraser, I., Manconi, F. and Gorrell, M. D. (2003). "3-dimensional imaging of collagen using second harmonic generation." J Struct Biol **141**(1): 53-62.

Cremazy, F. G., Manders, E. M., Bastiaens, P. I., Kramer, G., Hager, G. L., van Munster, E. B., Verschure, P. J., Gadella, T. J., Jr. and van Driel, R. (2005). "Imaging in situ protein-DNA interactions in the cell nucleus using FRET-FLIM." Exp Cell Res **309**(2): 390-6.

DeMali, K. A. and Burridge, K. (2003). "Coupling membrane protrusion and cell adhesion." J Cell Sci **116**(12): 2389-2397.

Denk, W., Strickler, J. H. and Webb, W. W. (1990). "Two-photon laser scanning fluorescence microscopy." Science **248**(4951): 73-6.

Diaspro, A. and Sheppard, C. J. R. (2002). Two-Photon Excitation Fluorescence Microscopy. Confocal and Two-Photon Microscopy: Foundations, Applications, and Advances. A. Diaspro. New York, Wiley-Liss, Inc.**:** 39-73.

Elenbaas, B., Spirio, L., Koerner, F., Fleming, M. D., Zimonjic, D. B., Donaher, J. L., Popescu, N. C., Hahn, W. C. and Weinberg, R. A. (2001). "Human breast cancer cells generated by oncogenic transformation of primary mammary epithelial cells." Genes Dev **15**(1): 50-65.

Eliceiri, K. W., Fan, C. H., Lyons, G. E. and White, J. G. (2003). "Analysis of histology specimens using lifetime multiphoton microscopy." J Biomed Opt **8**(3): 376-80.

Eliceiri, K. W. and Rueden, C. (2005). "Tools for visualizing multidimensional images from living specimens." Photochem Photobiol **81**(5): 1116-22.

Flusberg, B. A., Cocker, E. D., Piyawattanametha, W., Jung, J. C., Cheung, E. L. and Schnitzer, M. J. (2005). "Fiber-optic fluorescence imaging." Nat Methods **2**(12): 941-50.

French, T., So, P. T., Weaver, D. J., Jr., Coelho-Sampaio, T., Gratton, E., Voss, E. W., Jr. and Carrero, J. (1997). "Two-photon fluorescence lifetime imaging microscopy of macrophage-mediated antigen processing." J Microsc **185 (Pt 3)**: 339-53.

Freund, I. and Deutsch, M. (1986). "Second-harmonic microscopy of biological tissue." Optics Letters **11**(2): 94-96.

Friedl, P., Hegerfeldt, Y. and Tusch, M. (2004). "Collective cell migration in morphogenesis and cancer." Int J Dev Biol **48**(5-6): 441-9.

Friedl, P. and Wolf, K. (2003). "Tumour-cell invasion and migration: diversity and escape mechanisms." Nat Rev Cancer **3**(5): 362-74.

Galeotti, T., van Rossum, G. D., Mayer, D. H. and Chance, B. (1970). "On the fluorescence of NAD(P)H in whole-cell preparations of tumours and normal tissues." Eur J Biochem **17**(3): 485-96.

Goldberg, I. G., Allan, C., Burel, J. M., Creager, D., Falconi, A., Hochheiser, H., Johnston, J., Mellen, J., Sorger, P. K. and Swedlow, J. R. (2005). "The Open Microscopy Environment (OME) Data Model and XML file: open tools for informatics and quantitative analysis in biological imaging." Genome Biol **6**(5): R47.

Guo, Y. P., Martin, L. J., Hanna, W., Banerjee, D., Miller, N., Fishell, E., Khokha, R. and Boyd, N. F. (2001). "Growth factors and stromal matrix proteins associated with mammographic densities." Cancer Epidemiol Biomarkers Prev **10**(3): 243-8.

Hagios, C., Lochter, A. and Bissell, M. J. (1998). "Tissue architecture: the ultimate regulator of epithelial function?" Philos Trans R Soc Lond B Biol Sci **353**(1370): 857-70.

Hanahan, D. and Weinberg, R. A. (2000). "The hallmarks of cancer." Cell **100**(1): 57-70.

Harpur, A. G., Wouters, F. S. and Bastiaens, P. I. (2001). "Imaging FRET between spectrally similar GFP molecules in single cells." Nat Biotechnol **19**(2): 167-9.

Hegerfeldt, Y., Tusch, M., Brocker, E.-B. and Friedl, P. (2002). "Collective Cell Movement in Primary Melanoma Explants: Plasticity of Cell-Cell Interaction, {beta}1-Integrin Function, and Migration Strategies." Cancer Res **62**(7): 2125-2130.

Helmchen, F. and Denk, W. (2002). "New developments in multiphoton microscopy." Curr Opin Neurobiol **12**(5): 593-601.

Huang, S., Heikal, A. A. and Webb, W. W. (2002). "Two-photon fluorescence spectroscopy and microscopy of NAD(P)H and flavoprotein." Biophys J **82**(5): 2811-25.
Jacks, T. and Weinberg, R. A. (2002). "Taking the study of cancer cell survival to a new dimension." Cell **111**(7): 923-5.
Jaffe, A. B. and Hall, A. (2005). "RHO GTPASES: Biochemistry and Biology." Annual Review of Cell and Developmental Biology **21**(1): 247-269.
Jain, R. K., Munn, L. L. and Fukumura, D. (2002). "Dissecting tumour pathophysiology using intravital microscopy." Nat Rev Cancer **2**(4): 266-76.
Jung, J. C. and Schnitzer, M. J. (2003). "Multiphoton endoscopy." Opt Lett **28**(11): 902-4.
Katz, A., Savage, H. E., Schantz, S. P., McCormick, S. A. and Alfano, R. R. (2002). "Noninvasive native fluorescence imaging of head and neck tumors." Technol Cancer Res Treat **1**(1): 9-15.
Keely, P., Fong, A., Zutter, M. and Santoro, S. (1995). "Alteration of collagen-dependent adhesion, motility, and morphogenesis by the expression of antisense $\alpha 2$ integrin mRNA in mammary cells." J Cell Science **108**: 595-607.
Keely, P. J., Rusyn, E. V., Cox, A. D. and Parise, L. V. (1999). "R-Ras signals through specific integrin alpha cytoplasmic domains to promote migration and invasion of breast epithelial cells." J Cell Biol **145**(5): 1077-88.
Kirkpatrick, N. D., Zou, C., Brewer, M. A., Brands, W. R., Drezek, R. A. and Utzinger, U. (2005). "Endogenous fluorescence spectroscopy of cell suspensions for chemopreventive drug monitoring." Photochem Photobiol **81**(1): 125-34.
Lakowicz, J. R., Szmacinski, H., Nowaczyk, K., Berndt, K. W. and Johnson, M. (1992). "Fluorescence lifetime imaging." Anal Biochem **202**(2): 316-30.
Lee, K. C., Siegel, J., Webb, S. E., Leveque-Fort, S., Cole, M. J., Jones, R., Dowling, K., Lever, M. J. and French, P. M. (2001). "Application of the stretched exponential function to fluorescence lifetime imaging." Biophys J **81**(3): 1265-74.
Lin, E. Y., Jones, J. G., Li, P., Zhu, L., Whitney, K. D., Muller, W. J. and Pollard, J. W. (2003). "Progression to malignancy in the polyoma middle T oncoprotein mouse breast cancer model provides a reliable model for human diseases." Am J Pathol **163**(5): 2113-26.
Lippincott-Schwartz, J. and Patterson, G. H. (2003). "Development and use of fluorescent protein markers in living cells." Science **300**(5616): 87-91.
Lippincott-Schwartz, J., Snapp, E. and Kenworthy, A. (2001). "Studying protein dynamics in living cells." Nat Rev Mol Cell Biol **2**(6): 444-56.
Marsh, P., Burns, D. and Girkin, J. (2003). "Practical implementation of adaptive optics in multiphoton microscopy." Opt. Express **11**: 1123-1130.
Mohler, W., Millard, A. C. and Campagnola, P. J. (2003). "Second harmonic generation imaging of endogenous structural proteins." Methods **29**(1): 97-109.
Muti, P. (2004). "The role of endogenous hormones in the etiology and prevention of breast cancer: the epidemiological evidence." Ann N Y Acad Sci **1028**: 273-82.
Nazir, M. Z., Eliceiri, K. W., Ahmed, A., Hashmi, A., Agarwal, V., Rao, Y., Kumar, S., Lukas, T., Nasim, M., Rueden, C., Gunawan, R. and White, J. G. (2006). "WiscScan: A Software Defined Laser-Scanning Microscope." Scanning: Submitted.
Palmer, G. M., Keely, P. J., Breslin, T. M. and Ramanujam, N. (2003). "Autofluorescence spectroscopy of normal and malignant human breast cell lines." Photochem Photobiol **78**(5): 462-9.
Parsons, M., Monypenny, J., Ameer-Beg, S. M., Millard, T. H., Machesky, L. M., Peter, M., Keppler, M. D., Schiavo, G., Watson, R., Chernoff, J., Zicha, D., Vojnovic, B. and Ng, T. (2005). "Spatially distinct binding of Cdc42 to PAK1 and N-WASP in breast carcinoma cells." Mol Cell Biol **25**(5): 1680-95.

Paszek, M. J., Zahir, N., Johnson, K. R., Lakins, J. N., Rozenberg, G. I., Gefen, A., Reinhart-King, C. A., Margulies, S. S., Dembo, M., Boettiger, D., Hammer, D. A. and Weaver, V. M. (2005). "Tensional homeostasis and the malignant phenotype." Cancer Cell **8**(3): 241-54.

Patterson, G. H., Knobel, S. M., Arkhammar, P., Thastrup, O. and Piston, D. W. (2000). "Separation of the glucose-stimulated cytoplasmic and mitochondrial NAD(P)H responses in pancreatic islet beta cells." Proc Natl Acad Sci U S A **97**(10): 5203-7.

Peter, M. and Ameer-Beg, S. M. (2004). "Imaging molecular interactions by multiphoton FLIM." Biol Cell **96**(3): 231-6.

Peter, M., Ameer-Beg, S. M., Hughes, M. K., Keppler, M. D., Prag, S., Marsh, M., Vojnovic, B. and Ng, T. (2005). "Multiphoton-FLIM quantification of the EGFP-mRFP1 FRET pair for localization of membrane receptor-kinase interactions." Biophys J **88**(2): 1224-37.

Pitts, J. D., Sloboda, R. D., Dragnev, K. H., Dmitrovsky, E. and Mycek, M. A. (2001). "Autofluorescence characteristics of immortalized and carcinogen-transformed human bronchial epithelial cells." J Biomed Opt **6**(1): 31-40.

Plotnikov, S. V., Millard, A. C., Campagnola, P. J. and Mohler, W. A. (2006). "Characterization of the myosin-based source for second-harmonic generation from muscle sarcomeres." Biophys J **90**(2): 693-703.

Poteryaev, D., Squirrell, J. M., Campbell, J. M., White, J. G. and Spang, A. (2005). "Involvement of the Actin Cytoskeleton and Homotypic Membrane Fusion in ER Dynamics in Caenorhabditis elegans." Mol. Biol. Cell **16**(5): 2139-2153.

Pradhan, A., Pal, P., Durocher, G., Villeneuve, L., Balassy, A., Babai, F., Gaboury, L. and Blanchard, L. (1995). "Steady state and time-resolved fluorescence properties of metastatic and non-metastatic malignant cells from different species." J Photochem Photobiol B **31**(3): 101-12.

Ramanujam, N. (2000). "Fluorescence spectroscopy of neoplastic and non-neoplastic tissues." Neoplasia **2**(1-2): 89-117.

Rangarajan, A., Hong, S. J., Gifford, A. and Weinberg, R. A. (2004). "Species- and cell type-specific requirements for cellular transformation." Cancer Cell **6**(2): 171-83.

Robu, V. G., Pfeiffer, E. S., Robia, S. L., Balijepalli, R. C., Pi, Y., Kamp, T. J. and Walker, J. W. (2003). "Localization of Functional Endothelin Receptor Signaling Complexes in Cardiac Transverse Tubules
10.1074/jbc.M304396200." J. Biol. Chem. **278**(48): 48154-48161.

Ronnov-Jessen, L., Petersen, O. W., Koteliansky, V. E. and Bissell, M. J. (1995). "The origin of the myofibroblasts in breast cancer. Recapitulation of tumor environment in culture unravels diversity and implicates converted fibroblasts and recruited smooth muscle cells." J Clin Invest **95**(2): 859-73.

Rueden, C., Eliceiri, K. W. and White, J. G. (2004). "VisBio: a computational tool for visualization of multidimensional biological image data." Traffic **5**(6): 411-7.

Sahai, E., Wyckoff, J., Philippar, U., Segall, J. E., Gertler, F. and Condeelis, J. (2005). "Simultaneous imaging of GFP, CFP and collagen in tumors in vivo using multiphoton microscopy." BMC Biotechnol **5**: 14.

Sato, N., Maehara, N. and Goggins, M. (2004). "Gene Expression Profiling of Tumor-Stromal Interactions between Pancreatic Cancer Cells and Stromal Fibroblasts
10.1158/0008-5472.CAN-04-0677." Cancer Res **64**(19): 6950-6956.

Shen, y. r. (1989). "Surface properties probed by second-harmonic and sum-frequency generation." Nature **337**(9): 519-525.

Skala, M. C., Squirrell, J. M., Vrotsos, K. M., Eickhoff, J. C., Gendron-Fitzpatrick, A., Eliceiri, K. W. and Ramanujam, N. (2005). "Multiphoton microscopy of endogenous fluorescence differentiates normal, precancerous, and cancerous squamous epithelial tissues." Cancer Res **65**(4): 1180-6.

Squirrell, J. M., Eggers, Z. T., Luedke, N., Saari, B., Grimson, A., Lyons, G. E., Anderson, P. and White, J. G. (2006). "CAR-1, a Protein That Localizes with the mRNA Decapping Component DCAP-1, Is Required for Cytokinesis and ER Organization in Caenorhabditis elegans Embryos 10.1091/mbc.E05-09-0874." Mol. Biol. Cell **17**(1): 336-344.

Squirrell, J. M., Wokosin, D. L., White, J. G. and Bavister, B. D. (1999). "Long-term two-photon fluorescence imaging of mammalian embryos without compromising viability." Nat Biotechnol **17**(8): 763-7.

Stoller, P., Kim, B. M., Rubenchik, A. M., Reiser, K. M. and Da Silva, L. B. (2002). "Polarization-dependent optical second-harmonic imaging of a rat-tail tendon." J Biomed Opt **7**(2): 205-14.

Strome, S., Powers, J., Dunn, M., Reese, K., Malone, C. J., White, J., Seydoux, G. and Saxton, W. (2001). "Spindle Dynamics and the Role of {gamma}-Tubulin in Early Caenorhabditis elegans Embryos." Mol. Biol. Cell **12**(6): 1751-1764.

Tadrous, P. J., Siegel, J., French, P. M., Shousha, S., Lalani el, N. and Stamp, G. W. (2003). "Fluorescence lifetime imaging of unstained tissues: early results in human breast cancer." J Pathol **199**(3): 309-17.

Tlsty, T. D. and Hein, P. W. (2001). "Know thy neighbor: stromal cells can contribute oncogenic signals." Curr Opin Genet Dev **11**(1): 54-9.

van Munster, E. B. and Gadella, T. W. (2005). "Fluorescence lifetime imaging microscopy (FLIM)." Adv Biochem Eng Biotechnol **95**: 143-75.

Verveer, P. J., Wouters, F. S., Reynolds, A. R. and Bastiaens, P. I. (2000). "Quantitative imaging of lateral ErbB1 receptor signal propagation in the plasma membrane." Science **290**(5496): 1567-70.

Wang, W., Goswami, S., Lapidus, K., Wells, A. L., Wyckoff, J. B., Sahai, E., Singer, R. H., Segall, J. E. and Condeelis, J. S. (2004). "Identification and testing of a gene expression signature of invasive carcinoma cells within primary mammary tumors." Cancer Res **64**(23): 8585-94.

Wang, W., Goswami, S., Sahai, E., Wyckoff, J. B., Segall, J. E. and Condeelis, J. S. (2005). "Tumor cells caught in the act of invading: their strategy for enhanced cell motility." Trends Cell Biol **15**(3): 138-45.

Wang, W., Wyckoff, J. B., Frohlich, V. C., Oleynikov, Y., Huttelmaier, S., Zavadil, J., Cermak, L., Bottinger, E. P., Singer, R. H., White, J. G., Segall, J. E. and Condeelis, J. S. (2002). "Single cell behavior in metastatic primary mammary tumors correlated with gene expression patterns revealed by molecular profiling." Cancer Res **62**(21): 6278-88.

West, R. B., Nuyten, D. S., Subramanian, S., Nielsen, T. O., Corless, C. L., Rubin, B. P., Montgomery, K., Zhu, S., Patel, R., Hernandez-Boussard, T., Goldblum, J. R., Brown, P. O., van de Vijver, M. and van de Rijn, M. (2005). "Determination of stromal signatures in breast carcinoma." PLoS Biol **3**(6): e187.

White, J. G., Amos, W. B. and Fordham, M. (1987). "An evaluation of confocal versus conventional imaging of biological structures by fluorescence light microscopy." J Cell Biol **105**(1): 41-8.

Williams, R. M., Zipfel, W. R. and Webb, W. W. (2005). "Interpreting second-harmonic generation images of collagen I fibrils." Biophys J **88**(2): 1377-86.

Wokosin, D. L., Squirrell, J. M., Eliceiri, K. E. and White, J. G. (2003). "An optical workstation with concurrent, independent multiphoton imaging and experimental laser microbeam capabilities." Review of Scientific Instruments **74**(1).

Wozniak, M. A., Desai, R., Solski, P. A., Der, C. J. and Keely, P. J. (2003). "ROCK-generated contractility regulates breast epithelial cell differentiation in response to the physical properties of a three-dimensional collagen matrix." J Cell Biol **163**(3): 583-95.

Wozniak, M. A., Kwong, L., Chodniewicz, D., Klemke, R. L. and Keely, P. J. (2005). "R-Ras controls membrane protrusion and cell migration through the spatial regulation of Rac and Rho." Mol Biol Cell **16**(1): 84-96.

Zhang, J., Campbell, R. E., Ting, A. Y. and Tsien, R. Y. (2002). “Creating new fluorescent probes for cell biology.” Nat Rev Mol Cell Biol **3**(12): 906-18.

Zipfel, W. R., Williams, R. M., Christie, R., Nikitin, A. Y., Hyman, B. T. and Webb, W. W. (2003). “Live tissue intrinsic emission microscopy using multiphoton-excited native fluorescence and second harmonic generation.” Proc Natl Acad Sci U S A **100**(12): 7075-80.

Zipfel, W. R., Williams, R. M. and Webb, W. W. (2003). “Nonlinear magic: multiphoton microscopy in the biosciences.” Nat Biotechnol **21**(11): 1369-77.

Zoumi, A., Yeh, A. and Tromberg, B. J. (2002). “Imaging cells and extracellular matrix in vivo by using second-harmonic generation and two-photon excited fluorescence.” Proc Natl Acad Sci U S A **99**(17): 11014-9.

Figure Text

Figure 1: Live mammary tumor. Combined MPE and SHG at λ_{ex} = 890 nm facilitates imaging of intact live mammary tumor tissue. Panel (a) represents six planes of a 30-plane z-stack acquired every 10 μm (i.e. 300 μm total stack) into the tumor that was rendered and oriented with VisBio. Panels (b)-(g) show the flat images for each corresponding imaging plane. Combined panels clearly show variations in endogenous cellular fluorescence as well as collagen surrounding and within the tumor validating the ability to image deep into live tissue and obtain meaningful information. Bar = 50 μm.

Figure 2: MPE and SHG signal separation in live tumor. Since MPE excitation follows classical energy loss behavior while SHG signals are conserved, filtering techniques can be employed to separate the two signals following excitation with the same wavelength. Following excitation of live mammary tumor tissue with a wavelength (λ_{ex} = 890 nm) that elicits both endogenous cellular fluorescence and SHG (a), the resultant emissions were separated using a 445 nm narrow band pass filter for SHG (b; pseudocolored green) and a 464 nm (cut-on) long pass filter for MPE (c; pseudocolored red). This approach allows clear visualization of the collagenous stroma (b) as well as stromal and tumor cells (c), while merging the two pseudocolored signals (d) helps reveal cell matrix interactions associated with the tumor-stromal interface. As such, the use of combined MPE/SHG has the potential to help identify and differentiate additional features that are not readily obtained with more traditional fluorescent microscopy techniques. Bar = 25 μm.

Figure 3: Multiphoton FLIM of live mammary tumor: Following excitation at 890 nm, lifetime data was collected for 60 seconds using the Optical Work Station (described in the *Instrumentation* section) and displayed as (a) intensity or (b) color mapped lifetimes (color bar 0 to 1.6 ns; red to blue)

for a two-term exponential model (see Eq. 3). The color mapping represents the weighted average of the short and long components: $\tau_m = (a_1\tau_1 + a_2\tau_2) / (a_1 + a_2)$, although the relative contribution of each component for cells in the tumor is shown in (c). Additionally, due to the fact that signals from collagen principally arise from the conserved SHG polarization the resulting signal has a theoretical lifetime of zero, which is supported by the fact that the majority of the collagen signal closely follows the instrumental response function.

Figure 4: Invasive breast carcinoma cells in 3D matrices. Highly invasive and migratory MDA-MB-231 breast carcinoma cells cultured within reconstituted 3D collagen matrices to further examine the utility of combined MPE/SHG to probe the cell-matrix interaction. After three hours in collagen gels (a-c), MDA-MB-231 cells expressing GFP-Vinculin form 3D matrix adhesions by presenting filopodia that interact with collagen fibers (arrows in (a)). As is shown in (b), this interaction can be highlighted by separating the SHG signal (445 nm narrow band pass filter; green pseudocolor) and the GFP signal (480-550 nm band pass filter; red pseudocolor), while (c) is a magnified region (dashed box) of (b) clearly demonstrating vinculin positive filopodia interacting with collagen fibers. After 24 hours in 3D collage matrices (d: transmitted light), MDA-MB-231(GFP-vinculin) cells have aligned collagen fibers with vinculin localization at the cell-matrix interface (e, f: GFP=green pseudocolor; SHG blue pseudocolor). Hence, simultaneous imaging of cellular processes and matrix organization and structure with combined MPE/SHG not only facilitates imaging of non-native and endogenous signals *in vivo*, but also provides a robust tool to study tumor-stromal interactions in live (unfixed, unstained, non-sectioned) cells *in vitro*, which can further our understanding of the *in vivo* condition. Bar (a-c) = 10 μm; Bar (d-f) = 25 μm.

Figure 5: Changes in breast tumor cell and matrix signals as a function of excitation wavelength. By increasing the excitation wavelength from 780 to 880 nm in 20 nm increments, changes in the intensity and localization of endogenous fluorescence as well the emergence of collagen SHG at 860-880 nm is detectable. Bar = 25 μm.

Figure 6: Fluorescent lifetime of NADH in T47D breast carcinoma cells. Two-photon excitation at 740 nm elicits endogenous fluorescence of NADH. Color mapping represents the weighted average of the short and long components: $\tau_m = (a_1\tau_1 + a_2\tau_2) / (a_1 + a_2)$; color bar = 0.4 to 3 ns, red to blue.

Figure 7: Fluorescent lifetime of MDA-MB-231 breast carcinoma cells in 3D. 890 nm excitation of MDA-MB-231 breast carcinoma cells in 3D collagen gels. The color map represents the weighted average of the two-term model components [$\tau_m = (a_1\tau_1 + a_2\tau_2) / (a_1 + a_2)$] and validates the ability to detect changes in cellular lifetime of highly invasive breast carcinoma cells within a 3D culture environment. Color bar = 100 to 500 ps, red to blue.

Figure 8: Combined MPE/SHG of GFP-cdc42 in MDA-MB-231 cells within 3D collagen matrices. Live cells within type I collagen gels were imaged with combined MPE/SHG at λ_{ex} = 890 nm. After six hours within 3D collagen gels differences in cell morphology and the cell matrix interaction could be detected as a function of cdc42 state. Cells expressing constitutively active cdc42 (b) were more spread and presented more cell protrusions than both control GFP cells (a) and dominant negative expressing cells (c). Additionally over-expression of wild type cdc42 resulted in cell protrusion (d), but were not as spread as cells expressing constitutively active cdc42 (e). Moreover, separation of the GFP signal (480-550 nm band pass filter; green pseudocolor) from SHG (445 narrow

band pass filter, blue pseudocolor), reveals increased cell matrix attachments in cdc42(61L) cells with cdc42 localized to cell protrusions that are interacting with the collagen matrix.

Figure 9: Fluorescent lifetime imaging of a GFP-tagged molecule elucidates novel subdomains within the plasma membrane. GFP fused to constitutively active R-Ras (GFP-R-Ras(38V)) was transfected into Cos 7 cells and imaged by MPLSM: a) intensity image and b) color map of the FLIM of GFP-R-ras(38V) mapped from 1500 to 2500 ns; blue to red. c) Blow up of plasma membrane region shown in (b). Note that GFP-R-Ras(38V) localizes to active regions of the plasma membrane, which appear uniform in intensity via MPE in (a), but map to distinct lifetime domains in (b) and (c). FLIM was collected at 900nm utilizing a 60X plan apo (Nikon) lens utilizing a lab-built MPLSM as described in (Bird et al. 2004; Bird et al. 2005).

Figure 10. FLIM of a lipophilic fluorescent molecule, filipin, reveals subdomains within the plasma membrane. Cos-7 cells were incubated in 50 μM of the cholesterol-binding fluorophore filipin for 30 mins in order to detect microdomains of high cholesterol within the plasma membrane. Multiphoton excitation images of two exemplar cells are shown on the left. Color mapped (7 to 17 ns; red to blue) images representing the fluorescence lifetime of filipin were generated (right panels). The lifetime of this fluorophore was uncharacteristically long (>16 ns) throughout the entire membrane, however there are subregions with distinguishable lifetimes that are not detectable with standard multiphoton microscopy. FLIM was collected at 900nm utilizing a 60X plan apo (Nikon) lens utilizing a lab-built MPLSM as described in (Bird et al. 2004; Bird et al. 2005).

Figure 11: Spectral-Lifetime Imaging Microscopy (SLIM) analysis of tumor sections. Utilizing a recently developed MPLSM system in the Laboratory for Optical and Computational Instrumentation spectral lifetime data was obtained from hematoxylin and eosin stained polyoma middle-T mammary

tumor sections. The emission spectra was separated into 10 nm components over 16 channels: a) intensity image, b) total FLIM signaling, and c-f) the 510, 520, 530, and 540 nm emission components of the emission spectrum, respectively. Color mapping represents the weighted average of the two-term model components [$\tau_m = (a_1\tau_1 + a_2\tau_2) / (a_1 + a_2)$] with the color bar extending from 0 to 5 ns; red to blue. Of particular note is the observation that the total signal appears largely as background (b), yet the 530 nm emission component (e) reveals a low lifetime for the stroma (yellow) and a longer lifetime for the tumor cells (mostly green and blue) indicating that narrowing the detection spectra range while removing adjacent spectral components, that are most likely contributing significant noise, allows imaging and analysis of otherwise masked information.

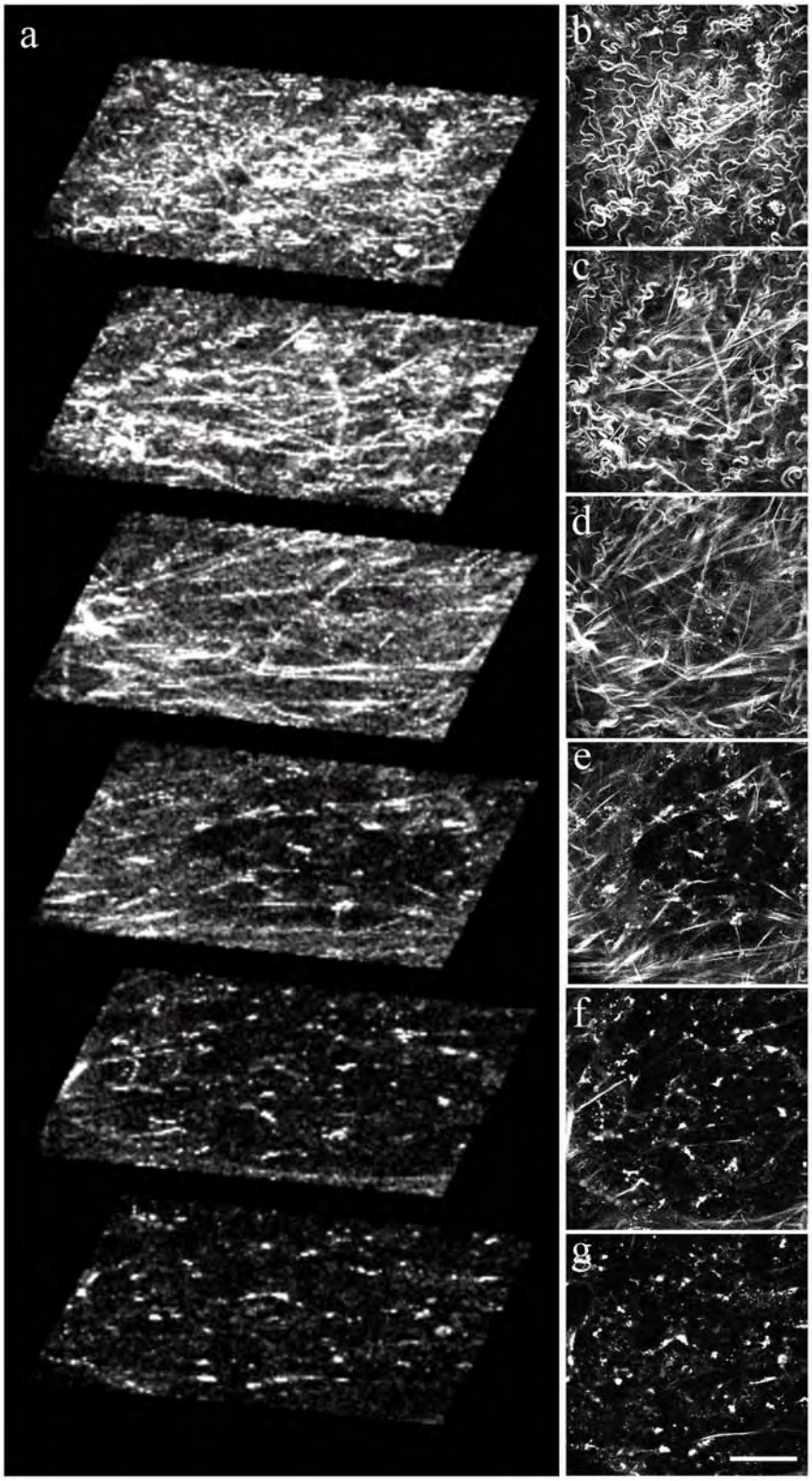

Fig. 1

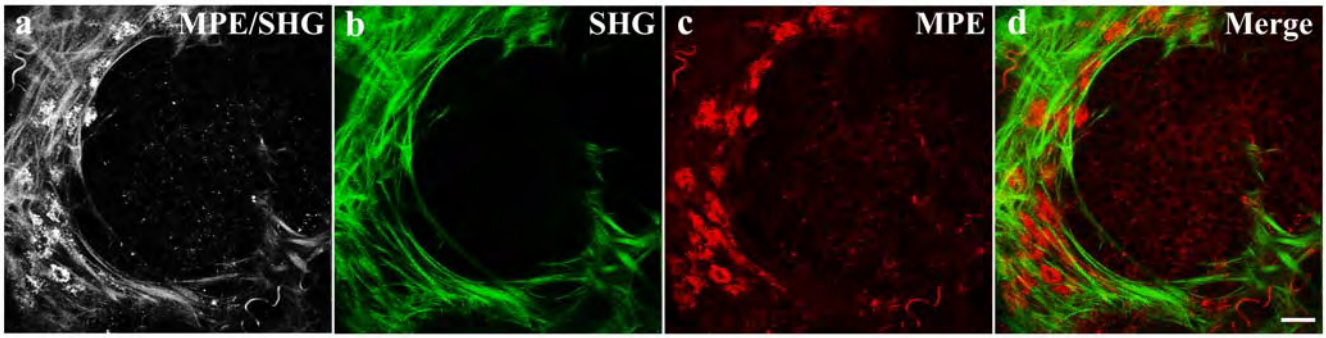

Fig 2

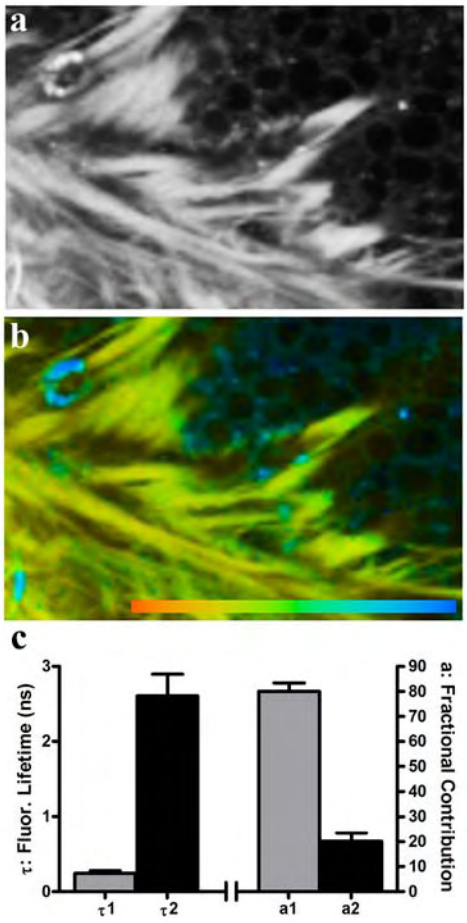
a
b
c
τ: Fluor. Lifetime (ns)
a: Fractional Contribution
0
1
2
3
0
10
20
30
40
50
60
70
80
90
τ1
τ2
a1
a2

Fig. 3

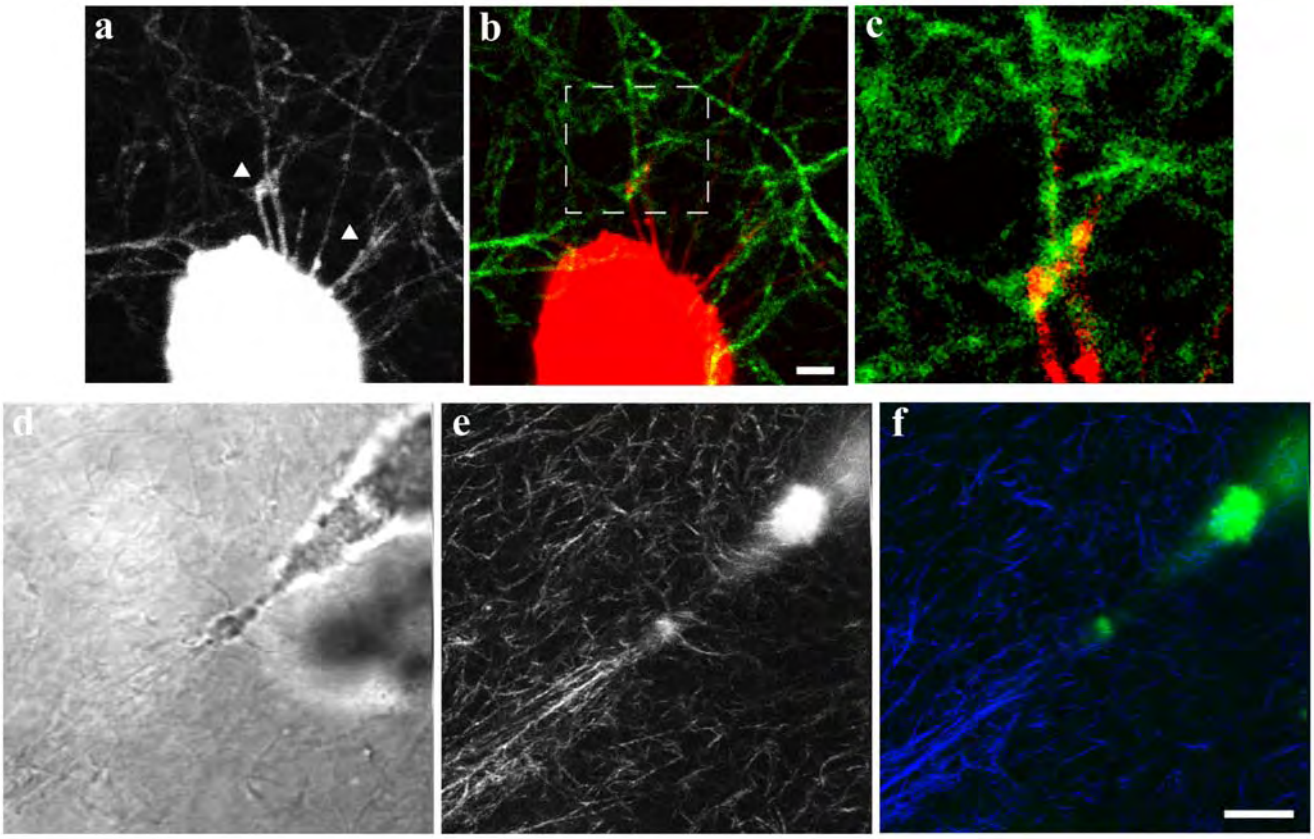

Fig. 4

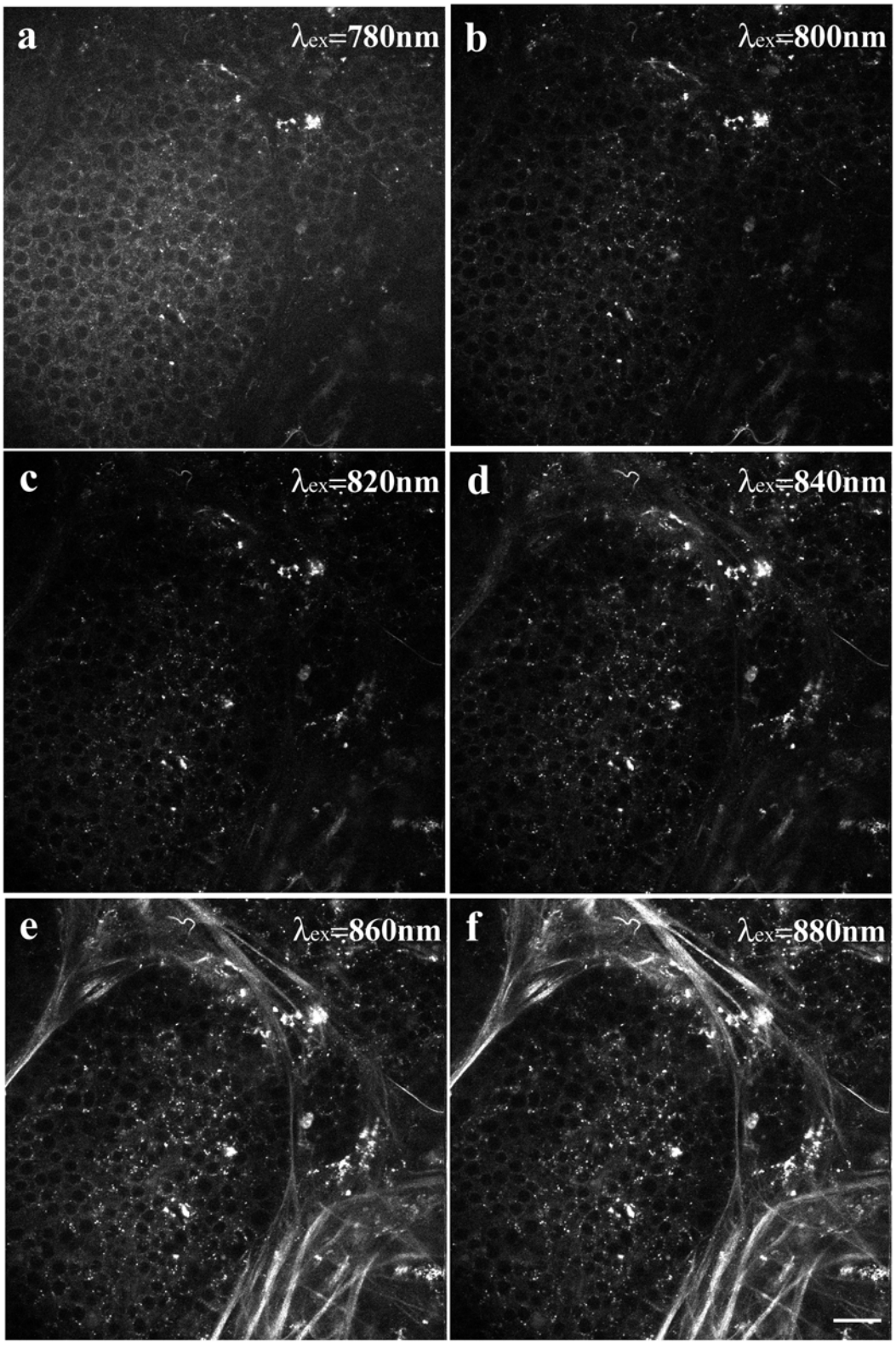
a
λex=780nm
b
λex=800nm
c
λex=820nm
d
λex=840nm
e
λex=860nm
f
λex=880nm

Fig. 5

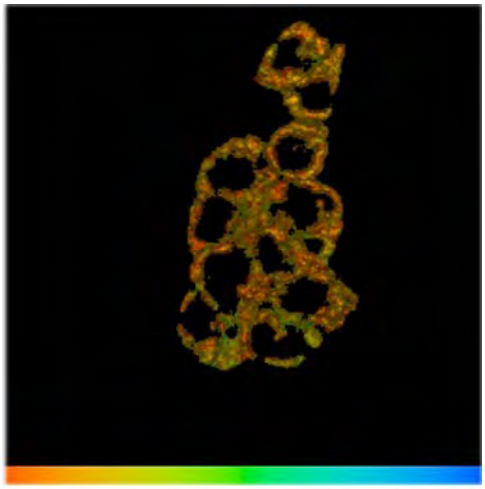

Fig. 6

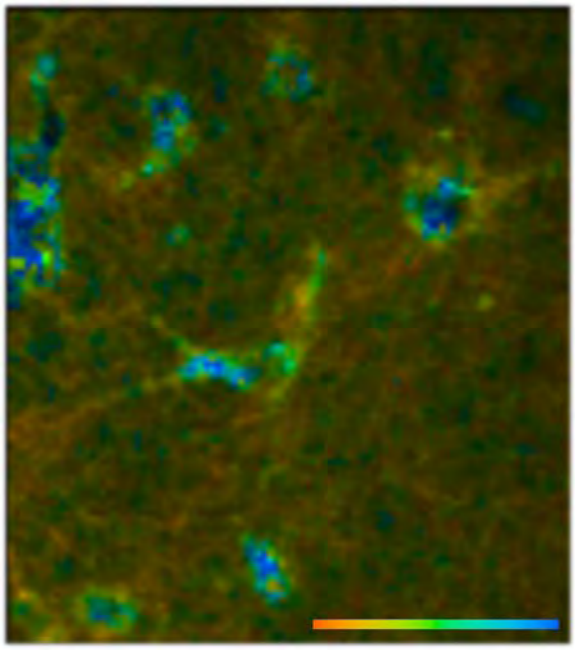

Fig. 7

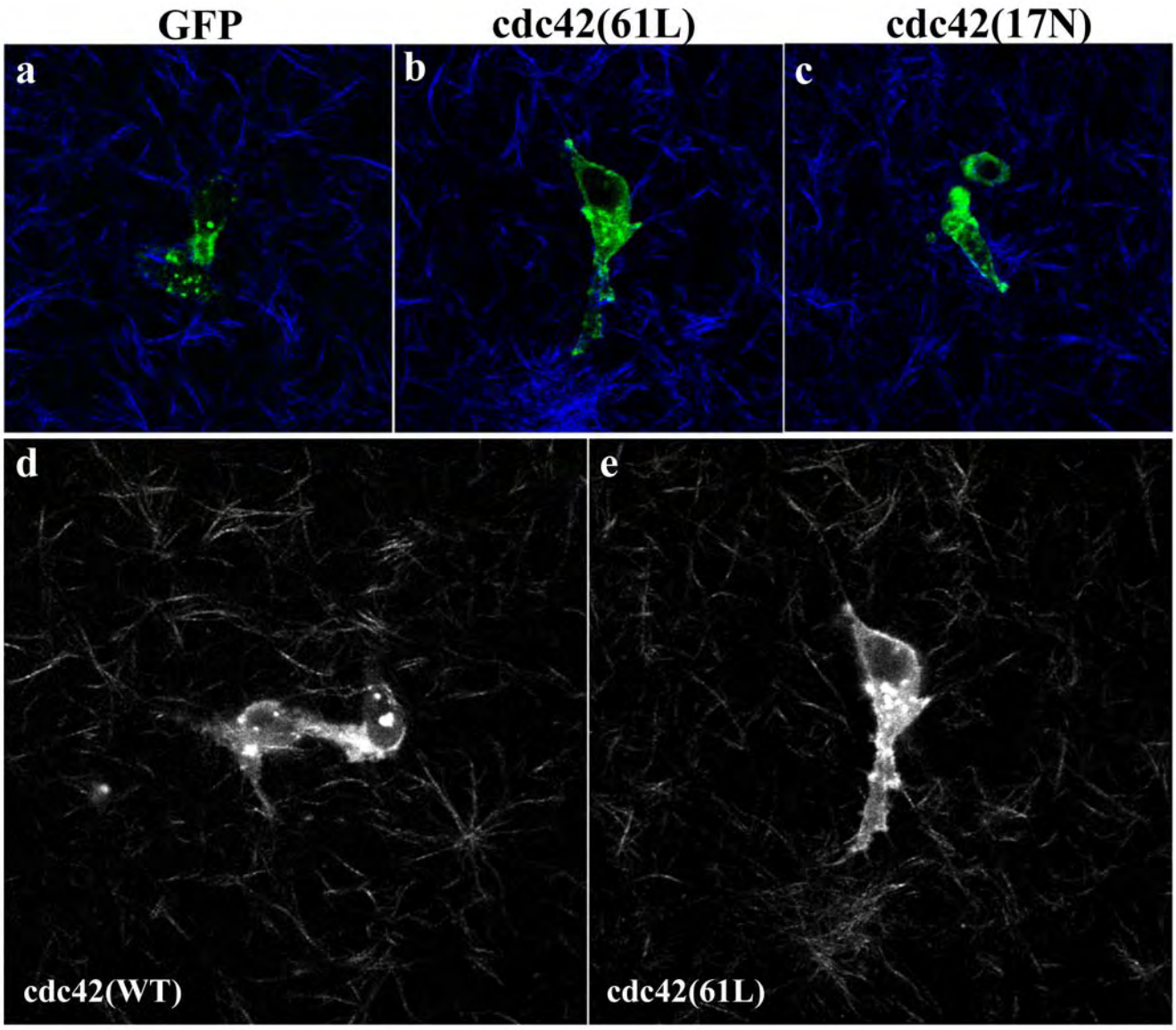

Fig. 8

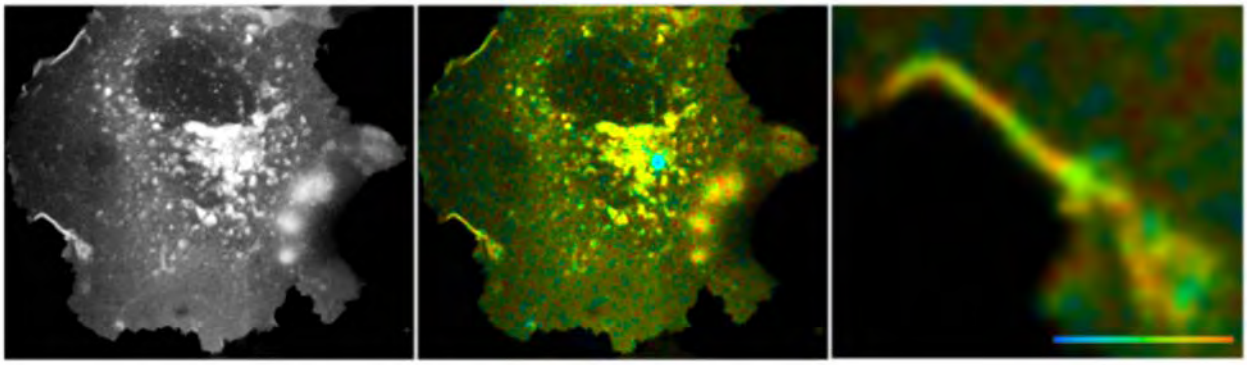

Fig. 9

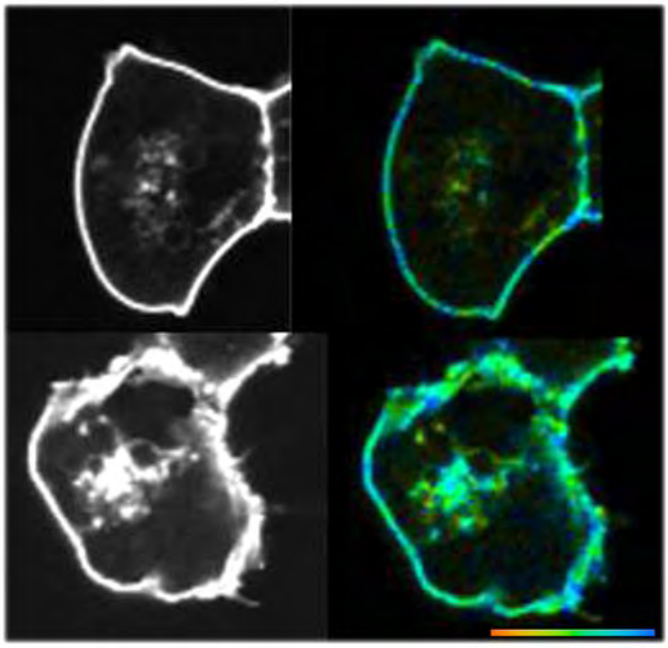

Fig. 10

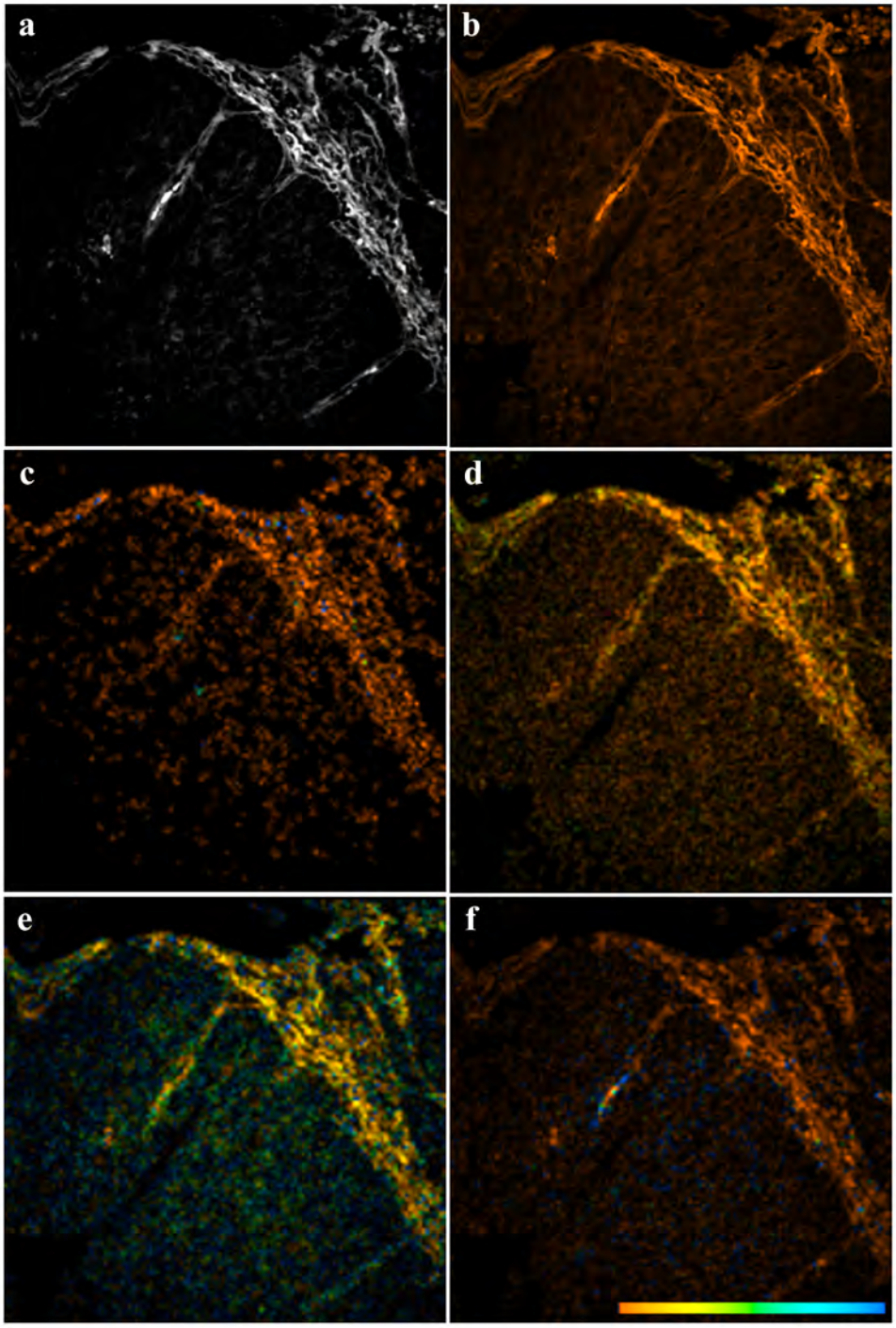

Fig. 11

Applications of combined spectral lifetime microscopy for biology

Long Yan, Curtis T. Rueden, John G. White, and Kevin W. Eliceiri

Laboratory for Optical and Computational Instrumentation
University of Wisconsin-Madison, Madison, WI, USA

Live cell imaging has been greatly advanced by the recent development of new fluorescence microscopy-based methods such as multiphoton laser-scanning microscopy, which can noninvasively image deep into live specimens and generate images of extrinsic and intrinsic signals. Of recent interest has been the development of techniques that can harness properties of fluorescence, other than intensity, such as the emission spectrum and excited state lifetime of a fluorophore. Spectra can be used to discriminate between fluorophores, and lifetime can be used to report on the microenvironment of fluorophores. We describe a novel technique—combined spectral and lifetime imaging—which combines the benefits of multiphoton microscopy, spectral discrimination, and lifetime analysis and allows for the simultaneous collection of all three dimensions of data along with spatial and temporal information.

Introduction

All living organisms are cells or ensembles of cells. This insight (1,2), arguably the most significant in all of biology, was made possible by the development of the light microscope (3). One hundred and sixty-seven years later, the microscope is still at the forefront of biomedical research into the structure and dynamics of subcellular components in living tissue. The remarkable developments in molecular biology and genomics during the past few years have provided DNA sequences of many organisms, from which the complete complement of proteins making up these organisms can be deduced. However, knowledge of a comprehensive "parts list" of an organism does little in and of itself to explain the workings of the dynamic machinery that underlies the ability of a cell to divide or differentiate. It is light microscopy that is providing the key insights into subcellular dynamics, a task being greatly facilitated by technical developments in optical probes and instrumentation. Chimeric fluorescent protein reporters (4–10) allow virtually any protein to be labeled and thereby visualized in a cell, tissue, or organism. Fluorescent molecules have been engineered to reveal key intracellular physiological parameters, such as free calcium levels (11–13). Along with these developments in fluorescence probe technology, new optical techniques, such as fluorescence resonance energy transfer (FRET) (14–17), multiphoton laser-scanning microscopy (MPLSM) (18–21), second harmonic generation (SHG) imaging (22–25), and fluorescence lifetime imaging (FLIM) (26–30), are revealing how individual cellular components are assembled into cytoplasmic machinery and how this machinery functions. In this review, we will describe a relatively new technique, spectral lifetime imaging microscopy (SLIM), that simultaneously measures fluorescence lifetime and spectra for intrinsic and extrinsic fluorophores. This technique can utilize the benefits of MPSLM and has great promise in revealing more information about intrinsic and extrinsic fluorophores and their interactions with each other and with their microenvironment.

MPLSM has proven to be a powerful tool for imaging cancer and cell biology phenomena (19,20,31–34) by allowing scientists to image noninvasively deep into biological tissue and collect four-dimensional data [three-dimensional (3-D) spatial dimensions plus time] of fluorescently labeled proteins. Recently, there has been a growing awareness that there are properties of fluorescence other than intensity, such as lifetime (how long a photon stays in the excited state) and spectra. These properties can be used to separate out fluorophores of interest (via spectra) and to reveal critical information about the microenvironment (via lifetime), as well as about the abundance and bound state of key endogenous fluorophores, such as nicotinamide adenine dinucleotide (NADH) (29,35) and flavin adenine dinucleotide (FAD). Until recently, all these dimensions of data have been collected separately, but now our group and others have developed instrumentation for simultaneous collection of intensity, space, time, spectra, and lifetime (36–38). This combined information can allow for the determination of the "fingerprint" of an intrinsic or extrinsic fluorophore in space and time, which allows investigators to track fluorophores accurately and determine their role in key processes.

Fluorescence Microscopy

Fluorescence microscopy has become the foremost tool in the study of the structure and dynamics of cellular machinery in living cells and tissue because of the high signal-to-background ratio that may be obtained by observing fluorescent objects against a black background, together with the ability to spectrally discriminate between mul-

tiple fluorophores, These fluorophores can be endogenous metabolites (e.g., reduced NADH), genetically engineered proteins [e.g., green fluorescent protein (GFP)::tubulin], or exogenous probes [e.g., fluorescence microscopy (FM) series lipid probes or the Ca^{2+} indicator Fura]. Each fluorophore has a characteristic emission spectrum that may be used for identification purposes. In addition, fluorophores have characteristic excited state lifetimes, which can be used also to aid identification (28). Excited state lifetimes—and, to a lesser extent, fluorescence spectra—can be modified by the microenvironment of the fluorophore and therefore can be used to report on it. By utilizing photon-counting detectors, the fluorescence lifetime of individual fluorophores, such as the bound and free forms of NADH, can be tracked and recorded for metabolic mapping in breast cancer (29).

Optical Sectioning Techniques

Optical sectioning techniques such as confocal laser-scanning microscopy (39,40) or MPLSM (19,21) have been developed that provide images from within a solid specimen that are free of interference from out-of-focus signals arising from fluorescent structures above and below the plane of focus. Stacks of optical sections can be collected enabling the 3-D structures of living specimens to be visualized over time (21,41,42). MPLSM is based on the nonlinear interactions between light and excitable molecules (21). At very high photon densities, two or more photons may be simultaneously absorbed by a fluorescent molecule causing it to fluoresce, provided the sum of the individual photon energies is equivalent to the energy required for a single photon to induce fluorescence. In the case of two-photon imaging, the excitation wavelength is set to about twice that of the absorption peak of the fluorophore being observed. Normally, this wavelength would not produce any appreciable excitation. However, if a high-power, ultrashort pulse laser is used, it is possible to achieve instantaneous photon densities that are sufficient to give rise to a significant yield of two-photon events in the focal volume (or focus scan area) of an objective lens, while maintaining a mean power level that will not damage the specimen. An additional advantage of MPLSM for in vivo studies is that phototoxic effects are minimized because fluorophore excitation is confined to the plane of the optical section being observed and longer wavelengths are utilized (21,43). Multiphoton imaging is the ideal instrumentation base for a SLIM system, as it provides the fluorescence excitation needed for spectral and lifetime collection, while retaining the viability and deep section benefits of MPLSM.

Fluorescence Lifetime Imaging

FLIM is a recently developed imaging mode where the excited state lifetimes of the fluorophores within a specimen are revealed (usually in false color) (28–31,44). The lifetime of the excited state, which gives rise to the emitted fluorescence photons, provides another dimension of information that is often independent of color. This extra dimension of data may be particularly useful in identifying fluorophores with significantly overlapping spectral properties. The excited-state lifetime is diagnostic of the fluorophore and also of its microenvironment (26,45). Factors such as ionic strength, hydrophobicity, oxygen concentration, binding to macromolecules, and the proximity of molecules that can deplete the excited state by resonance energy transfer can all modify the lifetime of a fluorophore. Measurements of lifetimes can therefore be used as indicators of these parameters. Fluorescence lifetime measurements are generally absolute, being independent of the concentration of the fluorophore. Lifetimes may be measured in either the frequency or time domains. We favor time domain measurements, because they use photon-counting techniques that minimize the effects of noise sources such multiplier gain noise in photodetectors and shot noise in analog amplifiers.

Spectral/Lifetime Multiphoton Imaging System

We have implemented a multiphoton imaging system that uses an innovative combined spectra/lifetime detector optimized for in vivo studies. When a fluorescence photon is emitted from a molecule within a living cell, it carries a signature that can potentially identify the molecule and provide information on the microenvironment in which it resides, thereby providing insights into the physiology of the cell. To unambiguously identify fluorescent probes and

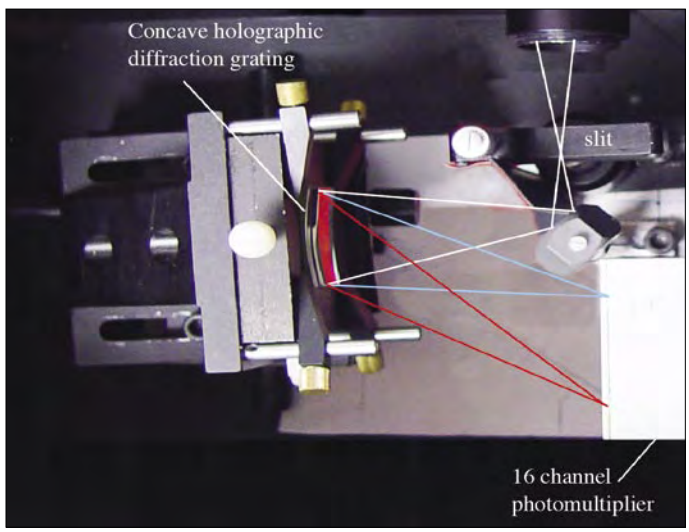

Figure 1. The spectrometer uses a concave, aberration-corrected holographic diffraction grating that provides a flat field and requires no auxiliary focusing optics. It is directly attached to the side-port of a Nikon Eclipse microscope via a condenser lens (not shown) that images the back aperture of the objective onto an adjustable slit. A mirror directs the beam onto the diffraction grating, which re-images the slit on the front face of the photomultiplier.

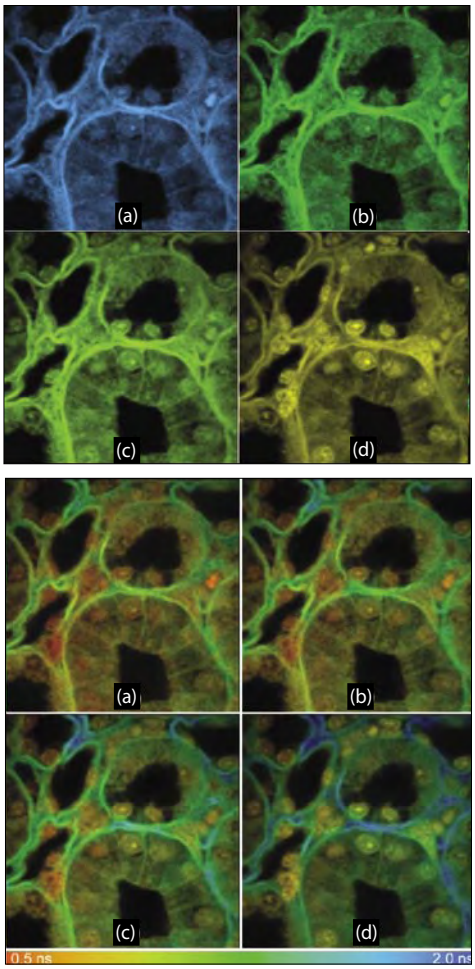

Figure 2. Multiphoton laser-scanning microscopy (MPLSM) spectral/lifetime images of a transverse section though the medulla of a Cynomolgus monkey kidney stained with methyl green. Top panel shows multiphoton intensity images acquired at the (a) 480 nm, (b) 510 nm, (c) 550 nm, and (d) 580 nm wavelength components of the emission spectrum, and bottom panel shows pseudocolor fluorescence lifetime images also acquired at the (a) 480 nm, (b) 510 nm, (c) 550 nm, and (d) 580 nm spectral intervals (±10 nm).

monitor their physiological environment within living specimens by their fluorescent signatures, one must exploit as much of this information as possible. Our combined two-photon spectral and lifetime microscope can collect fluorescence lifetime images from 16 individual wavelength components of the emission spectrum with 10-nm resolution on a pixel-by-pixel basis.

Our current spectrometer uses a blazed, aberration corrected, holographic diffraction grating (Shimadzu 20-046). These devices provide a flat field and so are ideally matched to a linear detector, requiring no additional focusing optics. Blazing has only recently been available on holographic gratings and has enabled efficiencies of >50% to be achieved around the blaze wavelength. The grating that we use has a wide f2 aperture, yet is small with a short (86 mm) focal length allowing a compact spectrometer to be designed that can be mounted directly on the side-port of a Nikon Eclipse TE2000-U microscope (Nikon, Melville, NY, USA) (Figure 1). Although this configuration loses some of the convenience of optical fiber coupling, we gain sensitivity as we can use a slit rather than a circular aperture for the spectrometer and also do not suffer any fiber coupling losses. The slit is adjustable so that trade-offs between spectral resolution and sensitivity can be made.

Examples of Biological Studies that Can Utilize SLIM

We have been exploring the possible application of spectral/lifetime imaging as a diagnostic tool for histologists to differentiate normal and malignant structures. In a pilot project, we have shown that FLIM can be used on classically stained histology slides to help differentiate between structures based on changes in lifetime (30). Initial studies have indicated that the extra dimensions of information provided by spectral/lifetime imaging could facilitate diagnostic judgments (Figure 2). We are now applying this work to standard hematoxylin and eosin (H&E) histopathology studies to investigate whether the extra information can facilitate the identification of diseased tissue from normal in standard path-lab specimens.

We have begun pilot studies in utilizing SLIM to study metabolism in breast cancer. Previous work demonstrated that FLIM can be utilized to detect the free and bound forms of NADH in human breast cell lines (29). We have now begun to utilize SLIM to look at NADH in both normal and malignant cell lines (Figure 3). The advantage of SLIM is that not only does it allow for detection of the free and bound forms of NADH via lifetime, but it also helps distinguish NADH from the other intrinsic fluorophores (such as FAD) via spectra.

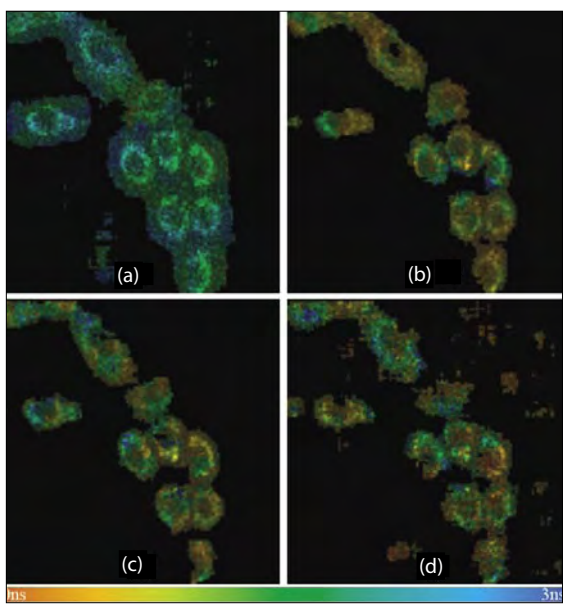

Figure 3. Multiphoton laser-scanning microscopy (MPLSM) spectral/lifetime images of live MCF10 breast cells. Panels depict lifetime images of the cells at the (a) 420 nm, (b) 440 nm, (c) 470 nm, and (d) 510 nm wavelength components of the emission range. Autofluorescence is from nicotinamide adenine dinucleotide (NADH), and cells were excited at 780 nm.

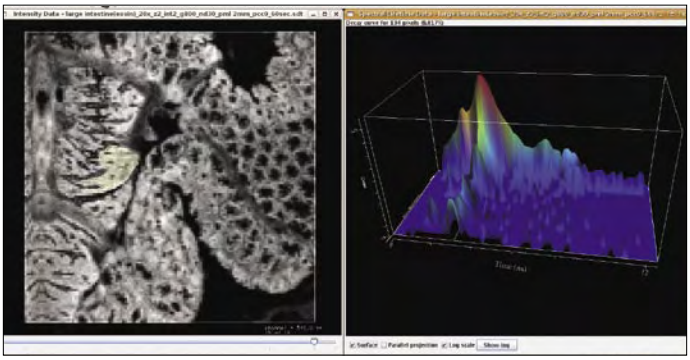

Figure 4. Pilot implementation of spectral lifetime imaging microscopy (SLIM) plotter application for spectral/lifetime visualization. The left panel displays an intensity image at each spectral channel (all lifetime bins summed together to produce an aggregate pixel value). A region of interest has been drawn by hand around pixels of interest, and the right panel shows a summed lifetime curve (along the time axis) at each spectral channel (wavelength axis) for the selected pixels. From the figure, it can be seen that the largest quantity of fluorescence took place across channels 14, 15, and 16 (approximate wavelength range 530–550).

Future Directions

The SLIM technique we have reported in this manuscript has great potential for cell biology applications. However, the limited photon counting rates of currently available instrumentation reduces the dynamic range of measurements and necessitates the use of long exposure times. This means that for some applications SLIM is impractical, as the photon-counting times needed are too long to capture the biological event in question. For widespread adoption, where scientists would routinely collect spectral and lifetime dimensions much in the same way that temporal and spatial dimensions are collected, great improvements in photon-counting electronics need to be made. New timing electronics have recently become available, so it is only a matter of time before these speed improvements are realized, allowing for shorter photon-counting times.

In addition to spectral and lifetime, fluorescence has another potentially useful property, polarization, which is the measure of the rotational state of the molecule. This property is, for the most part, not used in biology microscopy, but has great potential (16,46). Future systems could detect polarization for several types of studies including metabolic mapping of tumors (17) and measurements of receptor mobility in membranes (46).

Another ongoing challenge with SLIM is data analysis. The collection of simultaneous spectral and lifetime dimensions present practical challenges of how to store these data, due to their large size and complex structure. As well, there is the need for advanced approaches for mapping the data as quickly and effectively as possible. We have developed a software tool for performing analysis of combined spectral/lifetime data (Figure 4). It allows the specification of a freehand region of interest (ROI) to identify pixels of interest, then bins those pixels together to produce an aggregate lifetime decay curve for each spectral channel, plotting the results in an interactive 3-D window. We plan to introduce additional features into the software, such as the ability to bin multiple spectral channels together and export the results for use in other lifetime analysis products, such as the SPCImage program (Becker & Hickl GmbH, Berlin, Germany) for performing lifetime curve fitting.

Acknowledgments

This work was supported under National Institutes of Health (NIH) National Institute of Biomedical Imaging and BioEngineering (NIBIB) grant no. R01-EB000184.

References

1. **Schwann, T.** 1839. Mikroskopische Untersuchungen über die Übereinstimmung in der Struktur und dem Wachstum der Tiere und Pflanzen. Sander'schen Buchhandlung, Berlin.
2. **Scheiden, M.** 1838. Beitrfige zur Phytogenesis. Arch. Anat. Physiol. Wiss. Med. *13*:137-176.
3. **Mazzarello, P.** 1999. A unifying concept: the history of cell theory. Nat. Cell Biol. *1*:E13-E15.
4. **Zhang, S., C. Ma, and M. Chalfie.** 2004. Combinatorial marking of cells and organelles with reconstituted fluorescent proteins. Cell *119*:137-144.
5. **Zaccolo, M., F. De Giorgi, C.Y. Cho, L. Feng, T. Knapp, P.A. Negulescu, S.S. Taylor, R.Y. Tsien, and T. Pozzan.** 2000. A genetically encoded, fluorescent indicator for cyclic AMP in living cells. Nat. Cell Biol. *2*:25-29.
6. **Zaccolo, M. and T. Pozzan.** 2000. Imaging signal transduction in living cells with GFP-based probes. IUBMB Life *49*:375-379.
7. **Zacharias, D.A., G.S. Baird, and R.Y. Tsien.** 2000. Recent advances in technology for measuring and manipulating cell signals. Curr. Opin. Neurobiol. *10*:416-421.
8. **Zacharias, D.A. and R.Y. Tsien.** 2006. Molecular biology and mutation of green fluorescent protein. Methods Biochem. Anal. *47*:83-120.
9. **Tour, O., R.M. Meijer, D.A. Zacharias, S.R. Adams, and R.Y. Tsien.** 2003. Genetically targeted chromophore-assisted light inactivation. Nat. Biotechnol. *21*:1505-1508.
10. **Chalfie, M., Y. Tu, G. Euskirchen, W.W. Ward, and D.C. Prasher.** 1994. Green fluorescent protein as a marker for gene expression. Science *263*:802-805.
11. **Nakai, J., M. Ohkura, and K. Imoto.** 2001. A high signal-to-noise Ca(2+) probe composed of a single green fluorescent protein. Nat. Biotechnol. *19*:137-141.
12. **Yu, D., G.S. Baird, R.Y. Tsien, and R.L. Davis.** 2003. Detection of calcium transients in *Drosophila* mushroom body neurons with camgaroo reporters. J. Neurosci. *23*:64-72.
13. **Yu, R. and P.M. Hinkle.** 2000. Rapid turnover of calcium in the endoplasmic reticulum during signaling. Studies with cameleon calcium indicators. J. Biol. Chem. *275*:23648-23653.
14. **Tramier, M., I. Gautier, T. Piolot, S. Ravalet, K. Kemnitz, J. Coppey, C. Durieux, V. Mignotte, and M. Coppey-Moisan.** 2002. Picosecond-hetero-FRET microscopy to probe protein-protein interactions in live cells. Biophys. J. *83*:3570-3577.
15. **Miyawaki, A., J. Llopis, R. Heim, J.M. McCaffery, J.A. Adams, M. Ikura, and R.Y. Tsien.** 1997. Fluorescent indicators for Ca2+ based on green fluorescent proteins and calmodulin. Nature *388*:882-887.

16. **Gautier, I., M. Tramier, C. Durieux, J. Coppey, R.B. Pansu, J.C. Nicolas, K. Kemnitz, and M. Coppey-Moisan.** 2001. Homo-FRET microscopy in living cells to measure monomer-dimer transition of GFP-tagged proteins. Biophys. J. *80*:3000-3008.
17. **Rao, M. and S. Mayor.** 2005. Use of Forster's resonance energy transfer microscopy to study lipid rafts. Biochim. Biophys. Acta *1746*:221-233.
18. **Skala, M.C., J.M. Squirrell, K.M. Vrotsos, J.C. Eickhoff, A. Gendron-Fitzpatrick, K.W. Eliceiri, and N. Ramanujam.** 2005. Multiphoton microscopy of endogenous fluorescence differentiates normal, precancerous, and cancerous squamous epithelial tissues. Cancer Res. *65*:1180-1186.
19. **White, J., J.M. Squirrell, and K.W. Eliceri.** 2001. Applying multiphoton imaging to the study of membrane dynamics in living cells. Traffic *November*.
20. **Williams, R.M., W.R. Zipfel, and W.W. Webb.** 2001. Multiphoton microscopy in biological research. Curr. Opin. Chem. Biol. *5*:603-608.
21. **Denk, W., J.H. Strickler, and W.W. Webb.** 1990. Two-photon laser scanning fluorescence microscopy. Science *248*:73-76.
22. **Campagnola, P.J., A.C. Millard, M. Terasaki, P.E. Hoppe, C.J. Malone, W.A. Mohler.** 2002. Three-dimensional high-resolution second-harmonic generation imaging of endogenous structural proteins in biological tissues. Biophys. J. *82*:493-508.
23. **Campagnola, P.J., H.A. Clark, W.A. Mohler, A. Lewis, and L.M. Loew.** 2001. Second-harmonic imaging microscopy of living cells. J. Biomed. Opt. *6*:277-286.
24. **Zoumi, A., A. Yeh, and B.J. Tromberg.** 2002. Imaging cells and extracellular matrix in vivo by using second-harmonic generation and two-photon excited fluorescence. Proc. Natl. Acad. Sci. USA *99*:11014-11019.
25. **Williams, R.M., W.R. Zipfel, and W.W. Webb.** 2005. Interpreting second-harmonic generation images of collagen I fibrils. Biophys. J. *88*:1377-1386.
26. **Bastiaens, P.I. and A. Squire.** 1999. Fluorescence lifetime imaging microscopy: spatial resolution of biochemical processes in the cell. Trends Cell Biol. *9*:48-52.
27. **Pepperkok, R., A. Squire, S. Geley, and P.I. Bastiaens.** 1999. Simultaneous detection of multiple green fluorescent proteins in live cells by fluorescence lifetime imaging microscopy. Curr. Biol. *9*:269-272.
28. **Lakowicz, J.R., H. Szmacinski, K. Nowaczyk, K.W. Berndt, and M. Johnson.** 1992. Fluorescence lifetime imaging. Anal. Biochem. *202*:316-330.
29. **Bird, D.K., L. Yan, K.M. Vrotsos, K.W. Eliceiri, E.M. Vaughan, P.J. Keely, J.G. White, and N. Ramanujam.** 2005. Metabolic mapping of MCF10A human breast cells via multiphoton fluorescence lifetime imaging of the coenzyme NADH. Cancer Res. *65*:8766-8773.
30. **Eliceiri, K.W., C.H. Fan, G.E. Lyons, and J.G. White.** 2003. Analysis of histology specimens using lifetime multiphoton microscopy. J. Biomed. Opt. *8*:376-380.
31. **Parsons, M., J. Monypenny, S.M. Ameer-Beg, T.H. Millard, L.M. Machesky, M. Peter, M.D. Keppler, G. Schiavo, et al.** 2005. Spatially distinct binding of Cdc42 to PAK1 and N-WASP in breast carcinoma cells. Mol. Cell. Biol. *25*:1680-1695.
32. **Peter, M., S.M. Ameer-Beg, M.K. Hughes, M.D. Keppler, S. Prag, M. Marsh, B. Vojnovic, and T. Ng.** 2005. Multiphoton-FLIM quantification of the EGFP-mRFP1 FRET pair for localization of membrane receptor-kinase interactions. Biophys. J. *88*:1224-1237.
33. **Mohler, W.A. and J.G. White.** 1998. Multiphoton laser scanning microscopy for four-dimensional analysis of *C. elegans* embryonic development. Opt. Express *3*:325-331.
34. **Ahmed, F., J. Wyckoff, E.Y. Lin, W. Wang, Y. Wang, L. Hennighausen, J. Miyazaki, J. Jones, et al.** 2002. GFP expression in the mammary gland for imaging of mammary tumor cells in transgenic mice. Cancer Res. *62*:7166-7169.
35. **Lakowicz, J.R., H. Szmacinski, K. Nowaczyk, and M.L. Johnson.** 1992. Fluorescence lifetime imaging of free and protein-bound NADH. Proc. Natl. Acad. Sci. USA *89*:1271-1275.
36. **Bird, D.K., K.W. Eliceiri, C.H. Fan, and J.G. White.** 2004. Simultaneous two-photon spectral and lifetime fluorescence microscopy. Appl. Opt. *43*:5173-5182.
37. **Hanley, Q.S., D.J. Ardnt-Jovin, and T.M. Jovin.** 2002. Spectrally resolved fluorescence lifetime imaging microscopy. Appl. Spectrosc. *56*:155-166.
38. **Becker, W., A. Bergmann, E. Haustein, Z. Petrasek, P. Schwille, C. Biskup, L. Kelbauskas, K. Benndorf, et al.** 2006. Fluorescence lifetime images and correlation spectra obtained by multidimensional time-correlated single photon counting. Microsc. Res. Tech. *69*:186-195.
39. **White, J.G., W.B. Amos, and M. Fordham.** 1987. An evaluation of confocal versus conventional imaging of biological structures by fluorescence light microscopy. J. Cell Biol. *105*:41-48.
40. **Amos, W.B. and J.G. White.** 2003. How the confocal laser scanning microscope entered biological research. Biol. Cell. *95*:335-342.
41. **Thomas, C., P. DeVries, J. Hardin, and J. White.** 1996. Four-dimensional imaging: computer visualization of 3D movements in living specimens. Science *273*:603-607.
42. **Mohler, W.A. and J.G. White**. 1998. Stereo-4-D reconstruc tion and animation from living fluorescent specimens. BioTechniques *24*:1006-1012.
43. **Squirrell, J.M., D.L. Wokosin**, **J.G. White**, **and B.D. Bavister.** 1999. Long-term two-photon fluorescence imaging of mammalian embryos without compromising viability. Nat. Biotechnol. *17*:763-767.
44. **French, T., P.T. So, D.J. Weaver, Jr., T. Coelho-Sampaio, E. Gratton, E.W. Voss, Jr., and J. Carrero.** 1997. Two-photon fluorescence lifetime imaging microscopy of macrophage-mediated antigen processing. J. Microsc. *185*:339-353.
45. **Lin, H.J., P. Herman, and J.R. Lakowicz.** 2003. Fluorescence lifetime-resolved pH imaging of living cells. Cytometry A. *52*:77-89.
46. **Vishwasrao, H.D., A.A. Heikal, K.A. Kasischke, and W.W.Webb.** 2005. Conformational dependence of intracellular NADH on metabolic state revealed by associated fluorescence anisotropy. J. Biol. Chem. *280*:25119-25126.